Representing spatial variability of snow water equivalent in hydrologic and land-surface models: A review

Martyn P. Clark,[1] Jordy Hendrikx,[2] Andrew G. Slater,[3] Dmitri Kavetski,[4] Brian Anderson,[5] Nicolas J. Cullen,[6] Tim Kerr,[7] Einar Örn Hreinsson,[7] and Ross A. Woods[7]

Received 4 April 2011; revised 28 April 2011; accepted 3 May 2011; published 21 July 2011.

[1] This paper evaluates the use of field data on the spatial variability of snow water equivalent (SWE) to guide the design of distributed snow models. An extensive reanalysis of results from previous field studies in different snow environments around the world is presented, followed by an analysis of field data on spatial variability of snow collected in the headwaters of the Jollie River basin, a rugged mountain catchment in the Southern Alps of New Zealand. In addition, area-averaged simulations of SWE based on different types of spatial discretization are evaluated. Spatial variability of SWE is shaped by a range of different processes that occur across a hierarchy of spatial scales. Spatial variability at the watershed-scale is shaped by variability in near-surface meteorological fields (e.g., elevation gradients in temperature) and, provided suitable meteorological data is available, can be explicitly resolved by spatial interpolation/extrapolation. On the other hand, spatial variability of SWE at the hillslope-scale is governed by processes such as drifting, sloughing of snow off steep slopes, trapping of snow by shrubs, and the nonuniform unloading of snow by the forest canopy, which are more difficult to resolve explicitly. Subgrid probability distributions are often capable of representing the aggregate-impact of unresolved processes at the hillslope-scale, though they may not adequately capture the effects of elevation gradients. While the best modeling strategy is case-specific, the analysis in this paper provides guidance on both the suitability of several common snow modeling approaches and on the choice of parameter values in subgrid probability distributions.

Citation: Clark, M. P., J. Hendrikx, A. G. Slater, D. Kavetski, B. Anderson, N. J. Cullen, T. Kerr, E. Örn Hreinsson, and R. A. Woods (2011), Representing spatial variability of snow water equivalent in hydrologic and land-surface models: A review, *Water Resour. Res., 47*, W07539, doi:10.1029/2011WR010745.

1. Introduction

[2] Effectively representing the spatial variability of snow water equivalent (SWE) in hydrologic and land-surface models is critical in order to reliably simulate the basin-average snowmelt, as well as the energy and mass exchanges between the land and atmosphere [*Liston*, 1999]. This is because the spatial variability in snow accumulation and ablation processes controls the nonuniform disappearance of snow across the landscape. The nonuniform disappearance of snow is important from a hydrologic modeling perspective because it controls the magnitude, timing and duration of basin-average snow melt [*Lundquist and Dettinger*, 2004]. The nonuniform disappearance of snow is also important from a land-surface modeling perspective, as the presence/absence of snow and the patchiness of the snow cover strongly influence the radiative and turbulent heat fluxes between the land and atmosphere [e.g., *Cess et al.*, 1991; *Liston*, 1995; *Essery*, 1997]. The importance of this modeling challenge is matched by its difficulty, as the spatial variability in SWE is shaped by a range of different processes that occur across a hierarchy of spatial scales (e.g., the spatial variability in snow accumulation in alpine areas associated with preferential deposition of snow in microscale topographic depressions or in the lee of a ridge; the spatial variability in snow accumulation in forests associated with preferential deposition around fallen logs and spatial variability in interception and unloading of snow from the forest canopy; and the spatial variability in melt energy associated with local advection of energy across patchy snow covers and spatial variability in radiation loading and air temperature).

[3] Due to data limitations and computational constraints, spatial variability is typically handled in models by explicitly resolving only a few select levels in the hierarchy of spatial scales [*Kumar*, 2011]. Consider, for example, the

[1]National Center for Atmospheric Research, Boulder, Colorado, USA.
[2]Department of Earth Sciences, Montana State University, Bozeman, Montana, USA.
[3]Cooperative Institute for Research in Environmental Sciences, University of Colorado, Boulder, Colorado, USA.
[4]Environmental Engineering, University of Newcastle, Callaghan, New South Wales, Australia.
[5]Antarctic Research Centre, Victoria University of Wellington, Wellington, New Zealand.
[6]Department of Geography, University of Otago, Dunedin, New Zealand.
[7]National Institute of Water and Atmospheric Research, Christchurch, New Zealand.

0043-1397/11/2011WR010745

simulations of the transport and preferential deposition of snow over an alpine ridge performed by *Lehning et al.* [2008] and *Mott and Lehning* [2010], where the limited spatial extent of the model domain restricts analysis to processes at the hillslope scale. As another example, consider the representations of SWE developed by *Luce et al.* [1999] and *Liston* [2004], where probability distributions are used to parameterize the processes that occur below the resolved model scale. Since many different modeling strategies are possible, it is important to carefully consider their suitability in light of the available field data on the spatial variability of snow depth and SWE.

[4] The objective of this paper is to provide guidance to represent the spatial variability of SWE in hydrologic and land-surface models across a hierarchy of spatial scales. We pursue this objective by following three primary steps: (1) reanalyze results from previous studies on spatial variability in snow depth and SWE; (2) summarize a range of different approaches for multiscale representation of SWE; and (3) analyze the multiscale spatial variability in snow depth, as collected in a field campaign in the New Zealand mountains, and investigate the suitability of alternative modeling approaches.

2. Reanalysis of Results From Previous Studies

2.1. Sampling Design

[5] Table 1 summarizes the methods used in previous studies on the spatial variability in SWE, including a listing of the spacing, extent and support of the measurements, Figure 1 illustrates the locations of each of these studies. As defined by *Blöschl and Sivapalan* [1995] and *Blöschl* [1999], "spacing" refers to the distance between samples, "extent" refers to the overall coverage of the data, and "support" refers to the area represented by each sample. The previous work summarized in Table 1 is organized with respect to the classification of snow environments presented by *Liston* [2004].

[6] Table 1 demonstrates that previous studies differ substantially in terms of the support, spacing, and extent of the measurements.

[7] 1. The support in most studies is close to 0 (e.g., a single point measurement with a probe at each measurement location). Some studies do have larger support. For example, *Elder et al.* [1991] and *Balk and Elder* [2000] averaged measurements from the desired point as well as points 4 m away in the four cardinal directions, while the support can be viewed as 5 m, the distinction between spacing and support in this case is somewhat blurred. Sampling from radar [*Bruland et al.*, 2001; *Marchand and Killingtveit*, 2005] and terrestrial and airborne LiDAR [*Deems et al.*, 2006; *Grünewald et al.*, 2010] has larger support as radar measurements effectively average observations over the swath path of the radar, and LiDAR measurements effectively average over the cell size of the LiDAR.

[8] 2. The spacing between measurements is as small as 1.0–2.5 m for the radar and LiDAR studies [*Bruland et al.*, 2001; *Marchand and Killingtveit*, 2005; *Deems et al.*, 2006; *Trujillo et al.*, 2007; *Grünewald et al.*, 2010]. For manual snow measurements, spacing varies from a minimum of 5 m [*Erxleben et al.*, 2002; *McCartney et al.*, 2006] to a maximum of 50 m [*Balk and Elder*, 2000; *Winstral et al.*, 2002; *Erickson et al.*, 2005]. These larger spacings may actually be longer than the distance where the spatial correlation of snow depth is perceptible (i.e., longer than the correlation length scale), which can complicate the interpretation of the results.

[9] 3. The extent of measurements is quite variable, ranging from transects across a single snow drift [*Greene et al.*, 1999; *Sturm et al.*, 2001a], to intensive snow surveys in small basins such as the 0.26 km^2 Upper Sheep Creek catchment in Idaho, USA [*Luce et al.*, 1998, 1999], and the 0.32 km^2 Izas experimental catchment in the Spanish Pyrenees [*Anderton et al.*, 2004], to extensive surveys over larger regions, such as the radar survey in the 849 km^2 Aursunden basin in Norway [*Marchand and Killingtveit*, 2005]. The elevation range is negligible for studies conducted in flat areas [e.g., *Lapen and Martz*, 1996; *Shook and Gray*, 1996; *Faria et al.*, 2000] but is considerable in some of the studies conducted in mountainous terrain; for example, measurements taken by *Elder et al.* [1988] spanned 1351 vertical meters. Importantly, some studies in mountainous regions take measurements over only a limited elevation range, for example, measurements taken by *Anderton et al.* [2004] spanned only 215 vertical meters, thus limiting the extent to which accumulation and melt processes can be associated with variability in elevation.

[10] Clearly, the sampling design impacts on the results and hence complicates comparisons across different studies [see *Skoien and Blöschl*, 2006]. For example, since spatial variability generally increases with spatial scale [*Shook and Gray*, 1996; *Kutchment and Gelfan*, 2001], studies with limited spatial extent may underestimate the natural variability. Similarly, studies with large spacing between measurement points may not reveal the small-scale spatial correlation structures [*Balk and Elder*, 2000; *Winstral et al.*, 2002; *Erickson et al.*, 2005]. Nevertheless, in spite of the methodological differences, and the differences in relief/vegetation/climate, it is still possible to generalize some results from previous studies.

2.2. Dominant Processes

2.2.1. Controls by Drifting

[11] Many previous studies in nonforested environments suggest that drifting is the dominant process that affects spatial variability of snow depth. Here we define drifting to include preferential deposition of snow in sheltered areas during storms, as well as redistribution of snow by the wind from exposed to sheltered areas [e.g., *Lehning et al.*, 2008]. Drifting can be observed at multiple spatial scales, ranging from the micro scale (e.g., preferential deposition in topographic depressions) to the hillslope scale (e.g., preferential deposition in the lee of a ridge), to the watershed scale (e.g., preferential deposition on sheltered aspects).

[12] In a relatively flat area on the Canadian prairies (Kernen Research Farm near Saskatoon, Saskatchewan), *Shook and Gray* [1996] calculated the standard deviation of snow depth at sampling distances ranging from 1 m to 1 km and showed that the standard deviation within distances of ~30 m was just as large as the standard deviation at larger spatial scales. The principal feature at scales less than 30 m is snow dunes, which are formed by scour and redeposition of snow by wind. In another study on the Canadian prairies, *Lapen and Martz* [1996] produced maps of

Table 1. Summary of the Data Collection Strategies Used in Previous Studies

Environment	Region	References	Method	Number Samples	Support (m)	Spacing (m)	Extent (km^2)	Elevation Range	Vegetation Type
Midlatitude prairie	near Saskatoon, Saskatchewan, Canada	*Pomeroy et al.* [1993]	transect across a 4-meter tall Caragana hedge	~70	0	5	500 m transect	0	wheat stubble and fallow
Midlatitude prairie	southwest of Saskatoon, Saskatchewan, Canada	*Lapen and Martz* [1996]	depth sampled from a systematic grid of 756 locations, in 27 north-south transects through the site	756	0	30	1.5	22	wheat stubble, summerfallow , and uncut cereal crop
Midlatitude prairie	Kernen Farm and Strawberry Hill, Saskatchewan, Canada	*Shook and Gray* [1996]	transects along a relatively flat field of wheat stubble and fallow	2196	0	0.1--1.0	1	0	wheat stubble and fallow
Midlatitude flat forest	Harp Lake Four, near Huntsville, Ontario, Canada	*Buttle and McDonnell* [1987]	snowcourse across different forest types and aspects	32	not reported	not reported	not reported	not reported	mixed deciduous and coniferous forest
Midlatitude flat forest	Sleepers River, Vermont, USA	*Shanley and Chalmers* [1999]	SWE measured at ten sites within the catchment	10	0	not reported	111	581	Mix of northern hardwood forest and pasture
Midlatitude flat forest	Turkey Lakes watershed, central Ontario	*Murray and Buttle* [2003]	3 transects from clear-cut to forest, across the south-facing slope, across the ridge crest, and across the north-facing slope	55–78	0	5	~150 m transects	44	mixed hardwood forest (sugar maple and yellow birch) and clear-cuts
Midlatitude mountainous forest	Northern Colorado, USA	*Erxleben et al.* [2002]	each 1 km^2 Intensive Study Area (ISA) was subdivided into 100 m × 100 m grid cells, and snow depth measured at 5 points within each grid cell	550	0	5–25	1	53–251	mix of forest and clearing
Midlatitude mountainous forest	Glacier National Park, northern Montana, USA	*Geddes et al.* [2005]	SWE measured in six snow courses, with 4–6 sampling points each, extending from alpine tundra to subalpine forest on either side of a ridge	27	0	50–150	0.75 km^2	119	mix of subalpine forest and alpine tundra
Midlatitude mountainous forest	Interior Plateau, British Columbia, Canada	*Winkler and Moore* [2006]	sampling SWE at a regular 15 m × 15 m grid (8 points × 8 points) over an area of one hectare, in different vegetation types	576	0	15	0.1	0[a]	forest and open areas
Midlatitude mountainous forest	Northern Colorado, USA	*Deems et al.* [2006]; *Trujillo et al.* [2007]; *Deems et al.* [2008]	airborne LiDAR measurement of snow depth over 5 different 1 km^2 areas	1×10^6 for each area	1	1	1	53–235	mix of forest, meadow and alpine tundra
Midlatitude mountainous forest	Southeastern British Columbia, Canada	*Jost et al.* [2007]	sampling of snow depth and snow water equivalent across two perpendicular transects in 19 different strata	1480	0	2	17.4	1000	forest and open terrain
Midlatitude mountainous forest	Valles Caldera National Preserve, New Mexico	*Veatch et al.* [2009]	twenty 30 m × 30 m plots were subdivided into nine 10 m × 10 m subplots; snow depth was measured at 5 points within each subplot.	900	10	10	not reported	34	mix grassland, ponderosa pine, mixed conifer forest
Midlatitude mountainous forest	Little Deer Creek, Dry Creek Experimental Watershed, near Boise, Idaho, USA	*Homan et al.* [2011]	measurements every 50 m along a grid through 500 m^2 study area	121	0	50	0.25	210	mixed deciduous and evergreen forest
Midlatitude alpine	Schwangbach basin, Jura mountains, Switzerland	*Hosang and Dettweiler* [1991]	transect through the major axis of the river basin, measure snow water equivalent	33	5	100	2.1	-	wooded and open areas
Midlatitude alpine	Längental catchment, Tirol, Austria	*Blöschl et al.* [1991a]; *Blöschl et al.* [1991b]; *Blöschl and Kirnbauer* [1992]	oblique aerial photos taken 9 times during the ablation period	15,040[b]	25	25	9.4	1150	alpine

Table 1. (continued)

Environment	Region	References	Method	Number Samples	Support (m)	Spacing (m)	Extent (km^2)	Elevation Range	Vegetation Type
Midlatitude alpine	Emerald Lake basin, California, USA	*Elder et al.* [1991]	random sampling of snow depth from coordinates of a 25 m grid 4 times during the melt season[c]	86–354	5	25–100	1.2	616	exposed rock
Midlatitude alpine	Blackcap basin, California, USA	*Elder et al.* [1998]	12 transects scattered throughout the basin, ranging in length 400 900 m, with depth measured every 10 m.	709	0	10	92.8	1351	forest (lower slopes) and alpine veg (upper slopes)
Midlatitude alpine	Upper Sheep Creek, SW Idaho, USA	*Luce et al.* [1998]; *Luce et al.* [1999]	SWE measured at regular 30 m grid over basin 9 times during winter and spring.	247	0	30	0.26	200	shrub
Midlatitude alpine	Montgomery Pass, Medicine Bow Mountains, Colorado Rockies	*Greene et al.* [1999]	snow depth measured in an east-west transect across the ridge line	100	0	5	500 m transect	100	alpine tundra
Midlatitude alpine	Loch Vale basin, northern Colorado, USA	*Balk and Elder* [2000]	gridded depth sampling at the time of max accumulation. Used 50-m grid in uplands and 100 m grid in lowlands[d]	173–197	0–5	50–100	6.9	912	exposed rock and alpine vegetation
Midlatitude alpine	Green Lakes Valley, Colorado, USA	*Winstral et al.* [2002]; *Erickson et al.* [2005]	random sampling of snow depth from the coordinates of a 25 m grid at time of maximum accumulation	193–655	0	50	2.3	425	exposed rock, scree, alpine vegetation
Midlatitude alpine	Izas catchment, River Gállego, Spanish Central Pyrenees	*Anderton et al.* [2004]	transects of snow depth, supplemented with additional observations throughout the catchment	410	0	4	0.32	215	high mountain pasture with rock outcrops in steep areas
Midlatitude alpine	Albertibach catchment near Davos, Switzerland	*Grünewald et al.* [2010]	terrestrial scanning LiDAR	not reported	2.5	2.5	0.6	718	alpine area above tree line
Midlatitude alpine	Jollie River, Southern Alps, New Zealand	*Clark et al.* [2010]; this paper	26 manual transect surveys spread across characteristic aspects of the basin	2035	0.5	10	30	920	exposed rock, scree and alpine vegetation
High latitude flat forest	60-km E of Moosonee, northern Ontario	*Woo and Steer* [1986]	regularly spaced snow depth measurements in two 20 m × 40 m plots	356	0	~5	20 m× 40 m	0	spruce forest
High-latitude flat forest	Glenn Creek, near Fairbanks, Alaska	*Sturm* [1992]	measured tree-well profiles throughout winter for three spruce trees of different stem diameter	8–9 profiles for each tree	0	~0.05	2–5 m profiles	0	spruce forest
High-latitude flat forest	Tsaina River, 450 km South of Fairbanks, Alaska	*Sturm* [1992]	measured tree-well profiles for eleven spruce trees of different stem diameter	2–4 profiles for each tree	0	~0.05	1.0–2.5 m profiles	0	spruce forest
High-latitude flat forest	BOREAS SSA, near Saskatchewan	*Hardy et al.* [1997]	measured tree well profiles for 4 trees in the boreal jack pine forest	25	0	0.1	0.6	0	jack pine forest
High-latitude flat forest	Prince Albert National Park, Saskatchewan	*Faria et al.* [2000]	Ttansects of depth for different vegetation types	500	0	1	100 m transects	0	5 sites, mix of forest and clear-cut
High latitude mountainous forest	Aursunden, midsouth Norway	*Marchand and Killingtveit* [2005]	ground-based radar measurement in 9 sample snow fields at time of maximum accumulation	28,866–41,372	-	1	849[e]	863	mix of forest and alpine vegetation
High latitude alpine	Aursunden, min-south Norway	*Bruland et al.* [2004]	ground-based radar measurement in a grid pattern	16,700	-	1	1	0	above treeline: heather and lichen, with no taller vegetation

Table 1. (continued)

Environment	Region	References	Method	Number Samples	Support (m)	Spacing (m)	Extent (km^2)	Elevation Range	Vegetation Type
High latitude alpine	Wolf Creek Research Basin (near Whitehorse) Yukon, Canada	*Pomeroy et al.* [2004]	transects of depth and density along random-direction permanent snow courses, for different land cover types	25 points in each transect	0	~5	130 m transects	1550	mix of forest, shrub and alpine tundra
High latitude alpine	Granger basin, within Wolf Creek Research Basin (near Whitehorse) Yukon, Canada	*McCartney et al.* [2006]	transects of depth for different land cover types, monitored throughout the melt season	360[f]	0	5	8	650	shrub
High latitude alpine	Norefjell, southern Norway	*Skaugen* [2007]	single snow course visited every 14 days in the accumulation season and every 7 days in the melt season	200	0	10	2	0	
Arctic tundra	Spitzbergen, Svalbard	*Winther et al.* [1998]	radar measurements for longitudinal cross profiles across glaciers; measurement locations identified to minimize impacts of topography on accumulation	not reported	not reported	not reported	not reported	not reported	glaciers
Arctic tundra	Kuparuk basin, northern Alaska	*König and Sturm* [1998]	aerial photographs taken when about 50% of snow had melted, supplemented with depth observations in from a field traverse in 1996	15,400[g]	0	0.5	0.1[h]	-	tundra
Arctic tundra	Trail Valley Creek, Northwest Territories, Canada	*Essery et al.* [1999]	transects across Trail Valley Creek	not reported	0	not reported	not reported	not reported	shrub and open tundra
Arctic tundra	headwaters of the Toolik River, Alaska, USA	*Sturm et al.* [2001a]	transects perpendicular to a bluff edge over multiple years	not reported	0	not reported	not reported	20	tundra
Arctic tundra	near Happy Valley on the Dalton Highway, Alaska, USA	*Sturm et al.* [2001b]	measured snow properties through intersecting traverse lines through different vegetation types	567	0	not reported	several 1 km long transects	0	tussock tundra, shrubby tussock tundra, riparian shrub
Arctic tundra	Kuparuk basin, northern Alaska	*Liston and Sturm* [2002]	100 m transects at 71 sites from the headwaters of the Kuparuk basin to the Arctic coast	~14,000	0	0.5	19,550 km^2	1000	tundra
Arctic tundra	Arctic coastal plain, Alaska, USA	*Sturm and Liston* [2003]	100 m transects at 13 paired lake-nonlake stations	201 each transect	0	0.5	100 m transect	0	tundra
Arctic tundra	Ny-Ålesund, Svalbard	*Bruland et al.* [2001]	ground-based radar measurement in a grid pattern	~134,000; ~268,000	0	0.25	3 km^2 1998; 4 km^2 2000	not reported	tundra
Arctic tundra	Ny-Ålesund, Svalbard	*Bruland et al.* [2004]	ground-based radar measurement in a grid pattern	~134,000; ~268,000	0	0.25	3 km^2 1998; 4 km^2 2000	not reported	tundra
Arctic tundra	DeGeer valley, Svalbard	*Bruland et al.* [2004]	ground-based radar measurement for transects on the valley floor	~34,000	0	0.5	250 km^2	transects on valley floor	tundra
Arctic tundra	Imnavait Creek, headwaters of the Kuparuk River, Alaska, USA	*Homan et al.* [2011]	measurements every 50 m along a grid through 500 m^2 study area	121	0	50	0.25	20 m for site A, and 55 m for site B	tundra
Multiple landscape types	Finland	*Kuusisto* [1980]	grid of stakes, pine forest; grid of stakes, open fields	25; 9	0; 0	10; 5	50 m × 50 m; 15 m × 15 m	0; 0	pine forest and open fields
Multiple landscape types	not reported	*Pomeroy et al.* [1998]	monitor seasonal snow covers near the time of maximum accumulation	thousands	not reported	not reported	not reported	not reported	landscapes in the prairies, arctic, and the Boreal forest.

Table 1. (continued)

Environment	Region	References	Method	Number Samples	Support (m)	Spacing (m)	Extent (km^2)	Elevation Range	Vegetation Type
Multiple landscape types	former Soviet Union	*Kuchment and Gelfan* [2001]	transects of snow depth at various locations throughout the former Soviet Union	50–280	0	10–100	0.1-10	-	-
Multiple landscape types	Yellowstone National Park, NW Wyoming, USA	*Watson et al.* [2006]	measure SWE in a nested triangular configuration for different elevation, vegetation, and solar radiation classes	1222[i]	variable	variable	314	590	meadow, burned forest, pine forest

[a]Four sites were surveyed at an elevation of 1200 m and five sites were surveyed at a location of 1600 m.
[b]Number of cells = basin area (9,400,000 m^2)/cell size (625 m^2).
[c]In the 1988 season, only measured once at the time of maximum accumulation.
[d]Fewer samples were taken on the upper slopes due to time constraints.
[e]Used nine sample snow fields, with areas 4 km^2 and 9 km^2.
[f]Transect lengths are 120–275 m (nine transects). Assume mean transect length of 200 m and 40 points per transect (5 m spacing), then $n = 40 \times 9 = 360$.
[g]Number of depth samples = 200 samples for each of the 77 snow courses.
[h]Seventy-seven snow courses were visited, each of length 100 m.
[i]Sampled during seven different time periods.

snow depth that suggest statistical homogeneity at spatial scales greater than 100 m. Lapen and Martz explored relationships between spatial variability of snow depth and terrain attributes, and showed that snow depth is related to the terrain attributes that define sheltering by topographic obstacles. These results imply that drifting is a critical process in the Canadian Prairie environment.

[13] Drifting is the dominant process identified in studies conducted in small mountain catchments (<0.5 km^2) with limited elevation range (<250 m) and limited forest cover. *Greene et al.* [1999] took measurements in an East-West transect across a ridge line and measured elevated snow depths in drift less than 100 m wide. *Luce et al.* [1998, 1999] demonstrated for the Upper Sheep Creek in Idaho (area = 0.26 km^2, elevation range = 200 m; Table 1) that representation of snow drifting in models was essential in order to simulate the observed spatial pattern of SWE. *Anderton et al.* [2004] compared snow depth patterns with topographic indices in the Izas experimental catchment (area = 0.32 km^2, elevation range = 215 m), and demonstrated that variability in snow depth is negatively correlated with terrain exposure (i.e., positively correlated with sheltering). Anderton et al.'s regression tree models show that exposure indices explain most of the spatial variability in snow depth (see also the earlier work on sheltering indices by *Winstal et al.* [2002] as well as the subsequent work by *Dadic et al.* [2010] and M. Schirmer et al. (Persistence in intra-annual snow depth distribution: 1. Measurements and topographic control, submitted to *Water Resources Research*, 2011). More recently, *Mott et al.* [2011] illustrated that topographically modified wind fields and snow depth exhibited a similar scaling pattern, emphasizing the importance of wind in shaping the spatial variability of snow depth. In related studies, Schirmer et al. (submitted manuscript, 2011) and M. Schirmer and M. Lehning (Persistence in intra-annual snow depth distribution: 2. Fractal analysis of snow dept development, submitted to *Water Resources Research*, 2011) documented spatial and seasonal changes in scaling behavior of snow depth in which break distances were shown to depend on the underlying roughness of the terrain. An interesting result from the Schirmer and Lehning (submitted manuscript, 2011) study is that the scale break was shown to progressively increase throughout the accumulation season as smaller scale terrain features were buried by snow. In these small mountain catchments the spatial scale of drifting processes was less than 50 m.

[14] Drifting is also important in the Arctic tundra. *Sturm et al.* [2001a] made drift measurements over multiple years in the lee of a bluff in the headwaters of the Toolik River, Alaska, and documented snow depth in the drifts to be between 3000 and 4000 mm in all years, with a drift width typically less than 25 m. Such large depths of snow in the drift are remarkable given that the winter (September–May) precipitation in this region is typically between 100 and 150 mm. *Sturm and Liston* [2003] took detailed measurements of snow on paired sites on lakes and land throughout the Alaskan coastal plain and found snow depth to be much more variable on lakes than on land. They demonstrated that an initial irregular pattern of snow cover and lake ice is perpetuated by higher wind speed over the bare ice and lower wind speed over the snow cover, leading to the growth of snow dunes with characteristic lengths of 6 m.

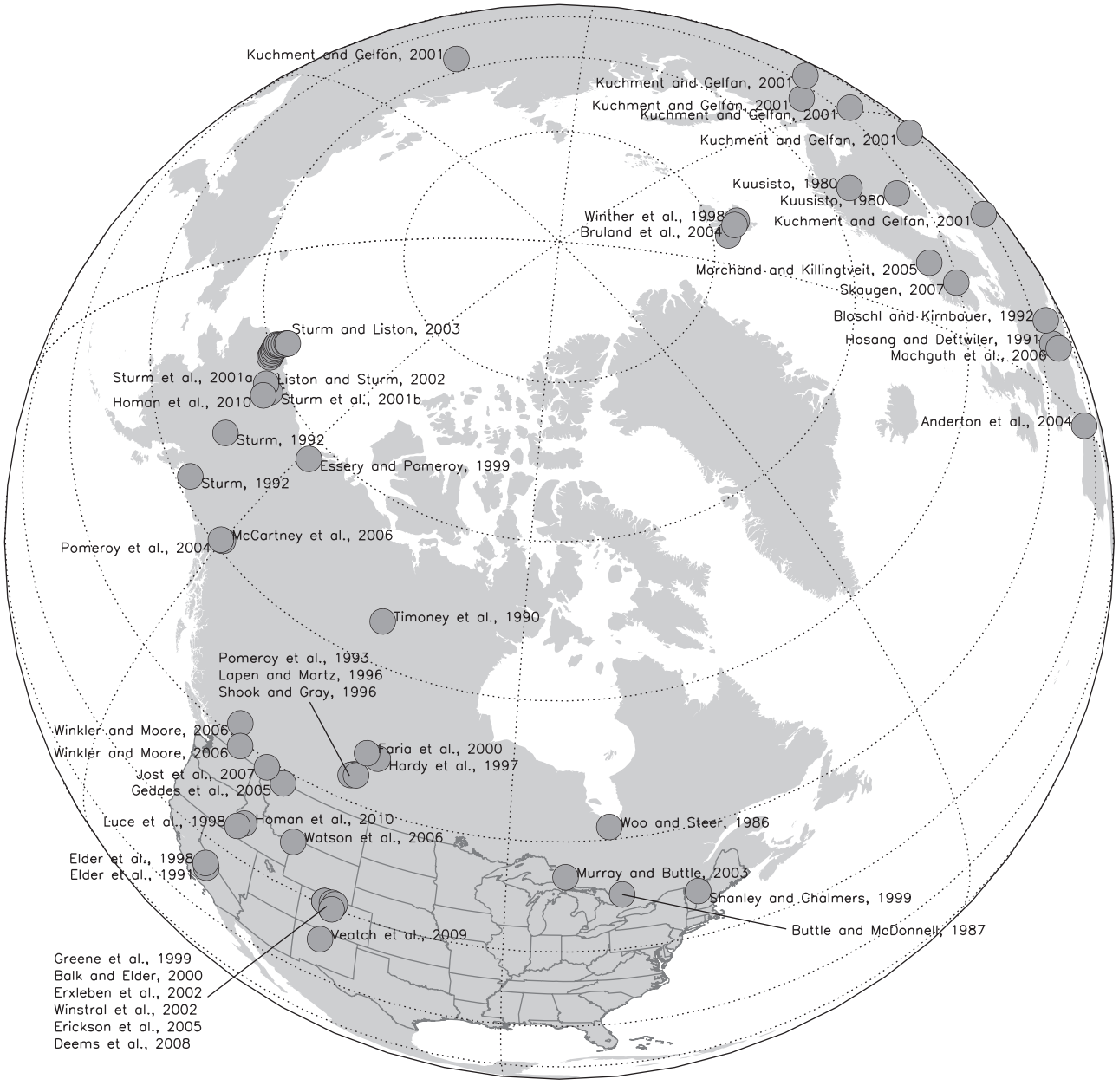

Figure 1. Location of previous field studies reviewed in this paper.

[15] Drifting is also important on sea ice. *Sturm et al.* [1998] demonstrated substantial spatial variability of snow depth on the west Antarctic pack ice, where depth on a single ice floe could vary almost as much as snow depth between different floes (the spatial distribution of snow depth was negatively skewed, with the standard deviation typically half the mean). Transects of snow depth across isolated pressure ridges revealed shallower depths on the ridge crest but deeper drifts of snow on both sides of the ridge; drifts of snow were typically confined to narrow strips 10–20 m wide. The addition of snow increased the topographic relief by accentuating larger-scale features such as pressure ridges but smoothed out the higher frequency surface roughness of ice by filling small depressions. In studies of snow depth on sea ice in the Canadian Arctic, *Iacozza and Barber* [1998] demonstrated substantial differences in the spatial distribution depending on ice type, with correlation length scales much larger for first-year sea ice than multiyear sea ice and rubble ice. While there was substantial variability within different ice types, much of this within-type variability could be explained by wind events and topographic structures, emphasizing the importance of drifting. In a subsequent study of the spatial variability of snow depth on sea ice in the Arctic Ocean, *Sturm et al.* [2002] documented similar spatial patterns to the earlier Antarctic study, with lower snow depth on ridge crests and drifts extending 15 to 25 m from the ridge crest in both directions. The spatial distribution of snow depth was also negatively skewed, with standard deviation approximately 60% of the mean.

[16] Drifting can be linked to the roughness of the terrain at multiple spatial scales. *Fitzharris*, [1977] carried out a

study of snow accumulation in traps at a range of scales on the block mountain terrain of Central Otago, New Zealand. His analysis included water stored behind (1) alpine vegetation; (2) tors; (3) breaks of slope; and (4) incipient cirques at fault scarps. *Fitzharris*, [1977] demonstrated that water stored behind vegetation was substantially larger than other storages, although once the snow depth exceeds the height of vegetation the trapping efficiency of vegetation is reduced to 0. In a later study, *Harrison* [1986] assessed controls of drifting in the Fraser catchment, Central Otago, New Zealand. He demonstrated that during milder winters, snow cover is irregular and the influence of microtopography is more pronounced. At larger spatial scales, aspect was important in controlling snow depth and snow water equivalent with over twice as much snow on sheltered slopes compared to those that were exposed. *Weir* [1979] diagnosed the topographic influences on snow accumulation at Mount Hutt, New Zealand. He showed that drifting had a large impact on SWE at spatial scales less than 1 m (drift deposits downwind of tussock) and at spatial scales of approximately 10 m (drift deposits in the lee of a ridge or in a gully). He also suggested that variability in SWE is related to aspect, to the extent that aspect defines sheltering from the prevailing winds.

2.2.2. Controls by Vegetation

[17] The impacts of vegetation on variability of snow depth are important in forest and shrub environments where the depth of snow is less than the height of the vegetation. An important distinguishing feature of spatial variability of snow depth in coniferous forests is the bowl-shaped depressions (tree wells) that from around the base of trees [*Woo and Steer*, 1986; *Sturm*, 1992; *Hardy et al.*, 1997; *Faria et al.*, 2000]. Tree wells form primarily because the branches intercept snow and restrict the amount of snow that can fall in the vicinity of the tree trunk; the snow intercepted by the upper crown cascades down through the branches with a tendency to move outward as it moves down [*Sturm*, 1992]. While the radius of tree wells depends on the size of the tree, tree well radii are typically less than 5 m [*Woo and Steer*, 1986; *Sturm*, 1992; *Hardy*, 1997; *Faria et al.*, 2000]. Spatial variability of snow depth in coniferous forests is also evident at the stand scale, as the interception and subsequent sublimation of snow from the forest canopy typically results in reduced snow accumulation under the forest canopy compared to open clearings [*Murray and Buttle*, 2003].

[18] An important control on the spatial variability of snow in forests is the interplay between accumulation and melt processes (e.g., see the recent review by *Varhola et al.* [2010]). At the stand scale, the reduced snow accumulation in forests is often offset by reduced melt, associated with both reductions in solar radiation caused by canopy shading and reductions in the sensible heat flux associated with canopy sheltering and attendant reductions in wind speed [*Hardy et al.*, 1997; *Link and Marks*, 1999a, 1999b; *Sicart et al.*, 2004; *Marks et al.*, 2008]. *Veatch et al.* [2009] demonstrated that the reduced melt under forest canopies can actually have a stronger impact than the sublimation losses from the forest canopy, meaning that snow depth is highest in stands with moderate canopy density. At finer spatial scales within a stand the competing effects of reduced accumulation and reduced melt may not apply. In the Canadian boreal forest, *Faria et al.* [2000] demonstrated that the lower premelt SWE near trunks had higher melt rates; they suggested that this negative correlation was due to a lower albedo near trunks because of greater leaf-litter concentration and energy advection from exposed plants. The spatial scale of snow depth variability in forests is often less than 40 m and is related to the size and spacing of trees [*Faria et al.*, 2000; *Pomeroy et al.*, 2002; *Jost et al.*, 2007; *Trujillo et al.*, 2007].

[19] In Arctic tundra environments shrubs influence the spatial variability of snow depth through trapping wind-blown snow [*Sturm et al.*, 2001; *Essery and Pomeroy*, 2004a; *McCartney et al.*, 2006; *Pomeroy et al.*, 2006]. *McCartney et al.* [2006] demonstrated that snow accumulation is highest in areas with tall shrubs, because tall shrubs create preferential areas for deposition of wind-blown snow. Shrubs also create preferential (albeit complex) patterns of ablation. *Pomeroy et al.* [2006] documented the complexities of snowmelt energetics in shrub tundra environments, showing that once shrubs were exposed they provided some shading of the snow surface, but that downward longwave radiation from the shrub canopy often exceeded the effect of attenuated shortwave transmission through the canopy. On the whole, *Pomeroy et al.* [2006] demonstrated that melt in shrub tundra environments was larger than melt in sparse tundra environments. The spatial scale of snow depth variability in the tundra is quite erratic and related to the distribution of vegetation types [*Essery and Pomeroy*, 2004a].

[20] The controls of exposure and vegetation often occur simultaneously. A set of studies in the midelevation Colorado mountains that use data collected during the NASA Cold Land Processes Experiment (CLPX) show that spatial variability of snow depth is almost as large at spatial scales of ~50 m than at larger spatial scales [*Erxleben et al.*, 2002; *Deems et al.*, 2006; *Trujillo et al.*, 2007]. *Trujillo et al.* [2007] demonstrated that in densely forested areas the scale of variability of snow depth was similar to the scale of variability of vegetation and suggested that interception of snow by the forest canopy is the dominant process affecting spatial variability of snow depth in forests. *Trujillo et al.* [2007] also demonstrated that in forest areas that are interspersed with open meadows the scale of variability of snow depth is larger than the scale of variability of vegetation. They suggested that scouring and redeposition of snow by wind leads to the formation of snow drifts and drifting is the dominant process affecting variability of snow depth in open areas. The CLPX snow depth data was collected over relatively homogenous areas [*Cline et al.*, 2009], so the limited variability at spatial scales greater than ~50 m is to some extent expected.

2.2.3. Controls by Freezing Levels and Melt Energy

[21] Controls on the spatial variability of snow at larger spatial scales have been investigated in a number of different rugged mountain environments [*Elder et al.*, 1998; *Balk and Elder*, 2000; *Winstral et al.*, 2002; *Erikson et al.*, 2005; *Grünewald et al.*, 2010]. *Elder et al.* [1998] used the variables of elevation, slope, and radiation loading in a regression tree model to predict spatial variability in SWE in the Blackcap basin, California (basin area = 92.8 km^2 and elevation range = 1351 m). Results were quite successful, with up to 65% of total variance explained for a 25 node model. *Elder et al.* [1988] demonstrate that slope angle plays a lesser role in explaining spatial variability in

snow depth than the variables elevation and radiation loading, which suggests that variability in freezing levels and radiative melt are the primary control on the spatial variability in SWE in this mountainous catchment.

[22] The oblique aerial photographs of snow cover presented by *Blöschl et al.* [1991a, 1991b] and *Blöschl and Kirnbauer* [1992] show strong relationships between snow cover and elevation and between snow cover and slope angle at spatial scales of ~500 m. They indicate that the relationships with elevation occur because of vertical variability in freezing levels and melt energy, whereas the relationships with slope angle occur because of sloughing and avalanching [*Blöschl and Kirnbauer*, 1992]. *Blöschl* [1999] constructed spatial variograms from these data, which show a large amount of variability is at spatial scales less than ~100 m. Some of this smaller-scale variability is likely related to the slope angle, attributed to the processes of sloughing and avalanching [*Blöschl and Kirnbauer*, 1992], and some of this smaller-scale variability is attributed to processes of wind drift as maps of terrain curvature indicated a tendency for less snow on ridges and more snow in gullies [*Blöschl and Kirnbauer*, 1992].

[23] *Machguth et al.* [2006] measured a strong elevation influence on snow depth on the lower part of the Findel Glacier in Switzerland which they attributed to variations in melt energy. However, on the upper part of the Findel and nearby Adler Glacier, accumulation was found to be much more variable and was attributed to wind redistribution.

[24] Several studies have demonstrated that the statistical models that rely on large-scale explanatory variables such as elevation and radiation loading can be improved through analysis of data at smaller spatial scales [*Balk and Elder*, 2000; *Winstral et al.*, 2002; *Erickson et al.*, 2005]. For example, *Winstral et al.* [2002] demonstrate improvement in their statistical model by adding wind drifting parameters. The additional model complexity represents processes that are dominant at spatial scales less than ~100 m, emphasizing multiscale variability in snow depth.

2.2.4. Controls at Multiple Spatial Scales

[25] A small number of studies present data on the variability of SWE at multiple spatial scales. *Marchand and Killingveit* [2005] examined radar data on snow depth variability in Åursunden (midsouth Norway) both *within* and *between* 30 m × 30 m grid cells. They show that the standard deviation in snow depth is slightly larger within grid cells than between grid cells. Attempts to use multiple linear regression models to predict between-grid variance were relatively ineffective (explained variance ranged between 5.6% and 48.6%), although elevation emerged as an important predictor in most regression models. Marchand and Killingveit's results emphasize variability at multiple spatial scales but provide few clues on the dominant processes that cause the variability at smaller spatial scales.

[26] *Watson et al.* [2006] used a stratified sampling scheme to study the variability in SWE in different landscape types in Yellowstone National Park, northwest Wyoming, USA. They decomposed spatial variability into a systematic component that could be predicted using covariates that are measureable at larger space-time scales (elevation, vegetation, radiation loading, time), and a random component that may be related to factors such as microtopography, fallen logs, distance from hollows around tree trunks, and small-scale wind effects. Measurements were taken in a triangular pattern at multiple spatial scales (1, 9, 100, 250, and 700 m). *Watson et al.* [2006] showed random effects were greatest at spatial scales less than 100 m. They also showed that variability associated with differences in elevation were approximately 3 times greater than the variability associated with random effects, but variability associated with differences in vegetation and radiation loading were approximately 3 times smaller than the variability associated with random effects.

[27] *Jost et al.* [2007] averaged SWE across 60 m × 60 m perpendicular transects, and then used the variables elevation, aspect, and forest cover to predict mean SWE at different transects throughout the basin. The coefficient of variation in SWE within transects ranged from 0.1 to 0.5 (depending on forest cover and the year of measurement; variability was smaller in clear-cuts), but, once this spatial variability is averaged out, regression models predicted over 80% of the variance in mean SWE. These results again emphasize that the variability in snow depth at different spatial scales is controlled by different processes.

2.3. Synopsis

[28] The subsequent discussion refers to four spatial scales, loosely defined as follows: (1) Point scale, which defines variability at scales less than 5 m associated with effects such as the roughness of the surface and the presence of an individual tree or shrub; (2) Hillslope scale, which defines variability at scales 1–100 m associated with effects such as topographic breaks and avalanching; (3) Watershed scale, which defines variability at scales 100–10,000 m associated with effects such as elevation and aspect; and (4) Regional scale, which defines variability at length scales ranging from 10 to 1000 km associated with effects such as horizontal precipitation gradients across a large mountain range. Regional-scale variability is not assessed in this paper, as we implicitly assume that regional scale variability will be explicitly resolved by distributed hydrologic and land-surface models. We do note, however, that heterogeneity at smaller spatial scales can impact the functional response of a watershed at larger spatial scales [e.g., see *Lundquist and Dettinger*, 2005; *Lundquist et al.*, 2005].

[29] Note that many snow processes will not fit neatly into any single scale category. For example, preferential deposition of snow is evident at the micro scale (in topographic depressions), at the hillslope scale (in the lee of a ridge), and at the watershed scale (sheltered aspects). Nevertheless, these general definitions can help organize results from previous studies.

[30] The dominant processes controlling variability in snow depth depend on the landscape and vegetation. Scour and redeposition of snow by wind is important in the Prairies and alpine areas [e.g., *Shook and Gray*, 1996; *Lapen and Martz*, 1996; *Mott et al.*, 2011; Schirmer et al., submitted manuscript, 2011], interception and sublimation of snow by the forest canopy (and spatial variability of radiative fluxes within the forest canopy) is important in the boreal forest [e.g., *Pomeroy et al.*, 2002], and trapping of snow by shrubs is important in the sub-Arctic tundra [e.g., *McCartney et al.*, 2006]. In mountain environments many processes act simultaneously to cause variability in snow depth: the dominant processes at the hillslope-scale are drifting [*Weir*,

1979; *Harrison*, 1986; *Luce et al.*, 1998; *Winstral et al.*, 2002; *Anderton et al.*, 2004; *Erickson et al.*, 2005; *Trujillo et al.*, 2007; *Fitzharris*, 1977], sloughing and avalanching [*Elder et al.*, 1991; *Blöschl and Kirnbauer*, 1992], and, where trees are present, interception and sublimation of snow by the forest canopy and spatial variability of radiative fluxes within the forest canopy [*Trujillo et al.*, 2007]. The dominant processes at the watershed scale in mountainous environments are variability in freezing levels and melt energy [*Elder et al.*, 1991; *Blöschl and Kirnbauer*, 1992; *Elder et al.*, 1998; *Watson et al.*, 2006].

[31] A subset of previous studies report summary statistics on the spatial variability of snow depth (or water equivalent). Figure 2 illustrates that the spatial variability in different regions is generally consistent with the estimates presented by *Liston* [2004]. The major exceptions to this generalization is that *Liston et al.* [2004] estimate lower spatial variability for the midlatitude nonmountainous forest, and higher spatial variability for the midlatitude mountainous forest. These differences are likely due to the sampling design (Table 1), in which studies in nonmountainous forest included open areas as well as forest, and the studies in mountainous forest generally covered only limited elevation range or report the spatial variability for subareas of the experimental domain. It is likely that the spatial variance in mountainous areas is actually higher than that presented in Figure 2 because steep slopes were under-sampled [e.g., *Balk and Elder*, 2000; *Erickson et al.*, 2005]. The outliers in Figure 2 include the studies of *Elder et al.* [1991], *Murray and Buttle* [2003] and *Watson et al.* [2006], who reported larger coefficient of variation values for very shallow snow depths at the end of the melt season. These results emphasize that the spatial variability in snow accumulation has a pronounced impact on area-averaged fluxes as the melt season progresses, leading to the development of patchy snow covers and slower area-average melt rates. Taken together, the synthesis of statistics in Figure 2 provides a useful guide to parameterize the spatial variability in SWE that is not resolved at the model scale.

[32] Table 2 summarizes the different process controls on snow depth variability gleaned from previous studies. The spatial separation of processes is quite blurred. For example, sloughing and avalanching can be viewed as processes that dominate at the hillslope scale (narrow avalanche paths), but sloughing and avalanching can have a vertical scale of thousands of meters. Conversely, spatial variations in melt energy can be viewed as important at the watershed scale, but variations in radiation loading associated with aspect can occur on spatial scales less than 100 m. Nevertheless, it appears that the processes that dominate at the hillslope scale (1–100 m) are different from the processes that dominate at the watershed scale (100–10,000 m).

3. Model Representations of Subgrid Variability in SWE

3.1. Subgrid Probability Distributions

[33] Parametric probability distributions can be used to represent the effects of spatial variability in SWE at the subgrid scale [*Luce et al.*, 1999; *Liston*, 2004; *Essery and Pomeroy*, 2004b]. For example, *Liston* [2004] used a log-normal probability distribution

$$f(S) = \frac{1}{S\zeta\sqrt{2\pi}} \exp\left\{ -\frac{1}{2}\left[\frac{\ln(S) - \lambda}{\zeta}\right]^2 \right\}, \tag{1}$$

with

$$\lambda = \ln(\mu) - \frac{1}{2}\zeta^2 \tag{2}$$

$$\zeta^2 = \ln\left(1 + CV^2\right), \tag{3}$$

where S is SWE, and λ and ζ are distribution parameters related to the mean (μ) and coefficient of variation (CV) of premelt SWE.

[34] *Luce et al.* [1999] and *Liston* [2004] assume that melt is spatially uniform over the grid cell, which means that the fractional snow covered area (F) and grid-average SWE ($\overline{S}$) can be computed as

$$F = \int_{D_m}^{\infty} f(S)\mathrm{d}S \tag{4}$$

$$\overline{S} = \int_{D_m}^{\infty} (S - D_m) f(S)\mathrm{d}S, \tag{5}$$

where D_m is the total melt since the beginning of the snow season.

[35] In this representation the mean of the premelt SWE distribution (μ) is taken as the sum of all accumulation events over the season. Implementing this method requires introducing two ancillary arrays that store the total snow accumulation (μ) and the total snow melt (D_m). Equations (4) and (5) can be solved analytically (see derivations in the work of *Liston* [2004]), thus saving the substantial computational cost of numerical integration.

[36] Figure 3 illustrates the reduction in fractional snow covered area (F) with increasing melt depth (D_m), and the corresponding relationships between F and normalized SWE ($\overline{S}/\mu$), for different CV parameters. Note that Figure 3a is identical to Figure 6a in the work of *Liston* [2004]. As shown in Figure 3a the larger CV parameters have the intended impact of reducing snow covered area at the start of the melt season (because of more areas of shallow snow that melt quickly) and increasing snow covered area at the end of the melt season (because of pockets of deep snow that persist well into summer). The appealing feature of using probability distributions to represent subgrid variability in SWE is that the parameters of the distribution (i.e., the CV parameter) can be estimated directly from observable data collected in field experiments such as those summarized in Figure 2.

[37] The assumption of spatially uniform melt is however questionable [*Luce and Tarboton*, 2004; *Essery and Pomeroy*, 2004b; *Pomeroy et al.*, 2004, 2008]. To illustrate the impact of this assumption we perform similar simulation experiments to those presented by *Essery and Pomeroy*

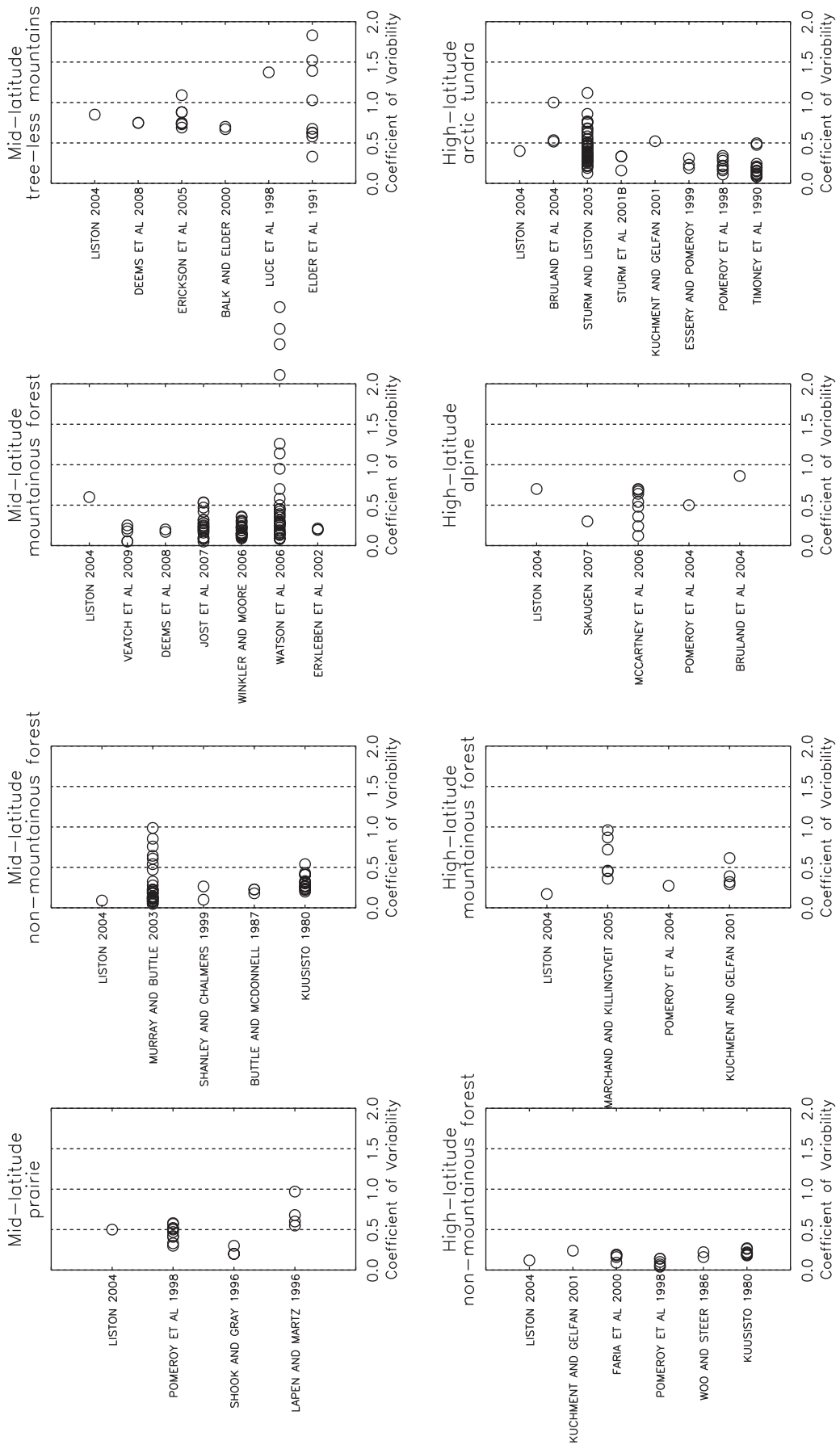

Figure 2. Coefficient of variability statistics documented in previous studies.

Table 2. Processes That Cause Spatial Variability in Snow Depth

Process	Predictors	Spatial Scale (m)	References
Variability in microtopography	-	1	*Watson et al.* [2006]
Snow interception/sublimation from the forest canopy	distance from trunk; spacing of trees; leaf area index	10	*Faria et al.* [2000]; *Pomeroy et al.* [2002]
Trapping of snow by tall shrubs	vegetation type	changeable	*Essery and Pomeroy* [2004a]; *McCartney et al.* [2006]; *Pomeroy et al.* [2006]
Preferential deposition of snow in sheltered areas and scouring and redeposition of snow by wind	sheltering indices	10–100	*Shook and Gray* [1996]; *Lapen and Martz* [1996]; *Luce et al.* [1998]; *Winstral et al.* [2002]; *Anderton et al.* [2004]; *Erickson et al.* [2005]; *Trujillo et al.* [2007]
Sloughing and avalanching	slope	10–1000[a]	*Elder et al.* [1991]; *Blöschl and Kirnbauer* [1992]
Variability in freezing levels	elevation	100–1000[b]	*Blöschl and Kirnbauer* [1992]; *Elder et al.* [1998]; *Balk and Elder* [2000]; *Winstral et al.* [2002]; *Marchand and Killingtveit* [2005]; *Watson et al.* [2006]
Variability in melt energy	elevation; slope; aspect; radiation loading	50–1000	*Elder et al.* [1991]; *Luce et al.* [1998]; *Balk and Elder* [2000]; *Watson et al.* [2006]

[a]The horizontal scale associated with sloughing and avalanching is often much smaller than the vertical scale.
[b]The horizontal scale associated with variability in freezing levels is often much larger than the vertical scale.

[2004b] and *Pomeroy et al.* [2008]. Here an initial lognormal premelt snow distribution ($\mu = 1$ m and $CV = 0.5$) is subjected to constant melt of 10 mm d^{-1} for 100 d). Three scenarios are tested: (1) melt is spatially uniform; (2) melt has moderate spatial variability, with standard deviation of 5 mm d^{-1}; and (3) melt has larger spatial variability with standard deviation of 10 mm d^{-1}. In scenarios 2 and 3 the spatial variability of melt is consistent over time, and melt values less than 0 were taken to be 0. The simulation results (Figure 4) illustrate that spatially

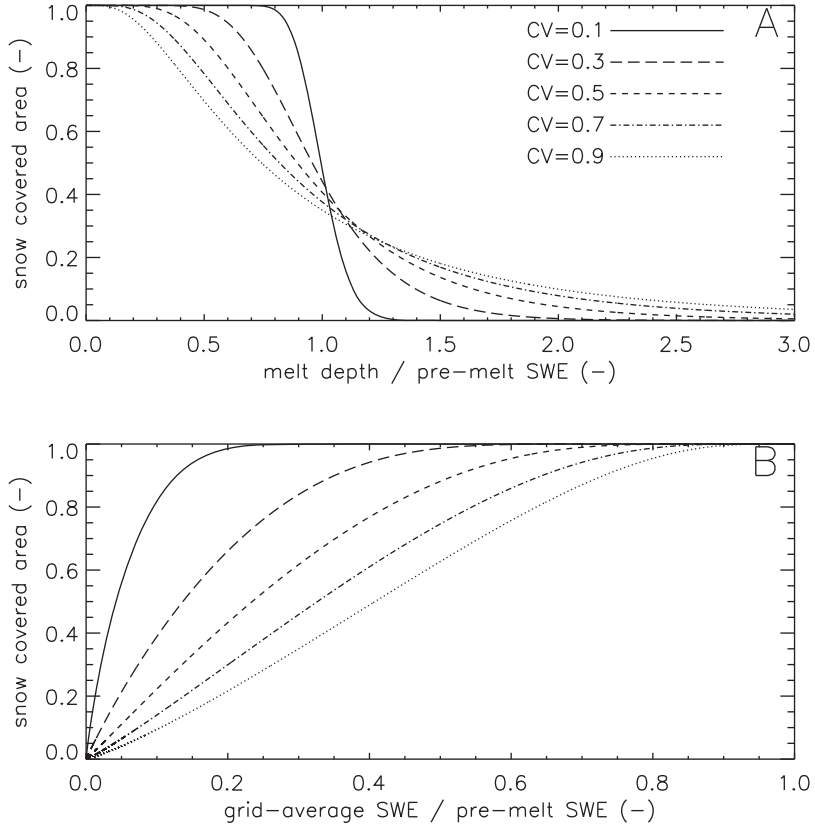

Figure 3. Behavior of subgrid SWE representations using probability distributions for the case of uniform melt, showing (a) the reduction of snow covered area with increasing melt depth, and (b) the functional relationship between SWE and snow covered area. Results are shown for different coefficient of variability parameters (see text for further details).

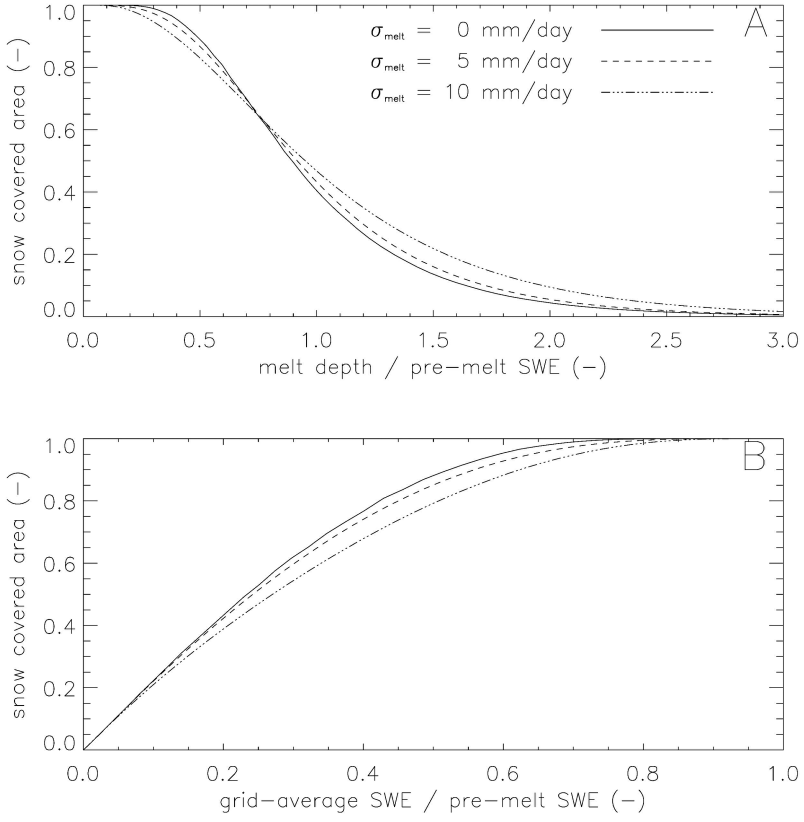

Figure 4. Behavior of subgrid SWE representations using probability distributions for the case of non-uniform melt, showing (a) the reduction of snow covered area with increasing melt depth, and (b) the functional relationship between SWE and snow covered area. Results are shown for the case where the coefficient of variability parameter is specified as 0.5.

variable melt has a similar impact on snow covered area to increased variability in premelt SWE. *Essery and Pomeroy* [2004b] demonstrate that these impacts are further accentuated in cases where the spatial variability in accumulation and melt are negatively correlated; a negative correlation between accumulation and melt means that melt rates for areas of shallow snow are larger than melt rates over areas of deep snow (i.e., areas of deeper snow melt more slowly).

3.2. Depletion Curves

[38] An alternative method used to represent the impacts of subgrid variability in SWE is to assume a relationship between SWE and snow covered area: the snow cover depletion curve. These depletion curves can have different functional forms; for example, see the comparison of different fractional snow covered area representations in Figure 2 of *Liston* [2004]. However, a problem with most depletion curves methods is that their parameters are not directly computable from observed data and hence are much harder to estimate.

[39] Consider the depletion curves used by *Yang et al.* [1997] and *Niu and Yang* [2007], given by

$$F = \tanh\left(\frac{\overline{S}_{\text{depth}}}{a}\right), \tag{6}$$

where F is the fractional snow covered area, $\overline{S}_{\text{depth}}$ is the grid-average snow depth (as opposed to SWE), and a is a parameter with the same dimensions as $\overline{S}_{\text{depth}}$ [see also *Essery and Pomeroy*, 2004b]. *Yang et al.* [1997] define a based on the aerodynamic roughness of the surface z_0^i,

$$a = 2.5\, z_0^i, \tag{7}$$

where i indexes the surface type (e.g., bare soil or grass), while *Niu and Yang* [2007] define a based on the roughness of the surface and snow density,

$$a = 2.5\, z_0^i \left(\frac{\rho_{\text{sno}}}{\rho_{\text{new}}}\right)^m, \tag{8}$$

where ρ_{sno} and ρ_{new} are the prognostic snow density and the density of fresh snow, respectively, and m is a melting factor that is adjustable depending on the spatial scale (the intent is that m should increase with spatial scale). Figure 5 illustrates the snow cover fraction representation of *Niu and Yang* [2007]; it shows that complete coverage of snow can occur with less than 10 cm of snow depth when snow density is low (e.g., 100 kg m^{-3}, typical of fresh snow), and larger fractions of snow free ground occur when snow density is higher (e.g., 400 kg m^{-3}, typical of a melting snowpack).

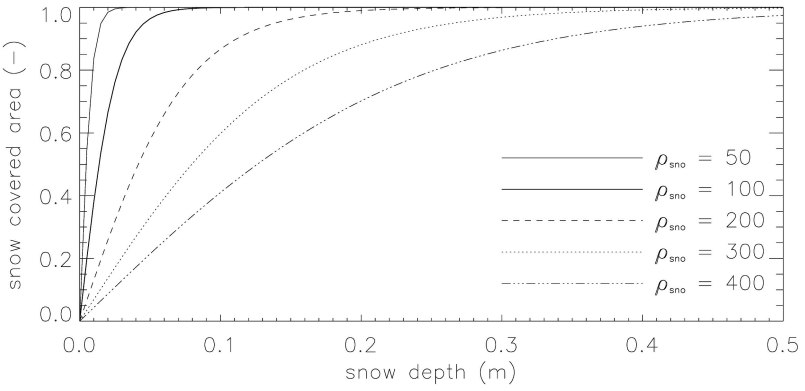

Figure 5. The subgrid SWE representation of *Niu and Yang* [2007], illustrated for different snow density values. The case where snow density is specified as 100 kg m^{-3} is identical to the subgrid SWE representation used by *Yang et al.* [1997].

[40] Despite the apparent physical basis of equations (6)–(8), depletion curves of this type contain nonobservable constants. For example, *Yang et al.* [1997] multiply surface roughness by 2.5, and Niu and Yang use an adjustable "melting factor" ($m = 1.6$). They are also further modified using heuristic arguments. For example, *Roesch et al.* [2001] argued that the *Yang et al.* [1997] parameterization is only valid over flat nonvegetated areas, and introduced an empirical modification for nonforested mountainous areas: the decrease in snow cover fraction with increasing subgrid variance in elevation is represented by multiplying the subgrid variance in elevation by a factor of 0.15. Similarly, *Essery and Pomeroy* [2004b] replace the dependence on surface roughness used by *Yang et al.* [1997] with a dependence on the standard deviation of premelt SWE but introduce empirical constants to match the depletion curves produced by subgrid probability distributions.

[41] These arguments suggest that subgrid probability distributions are a more appealing approach for most applications, because the *only* parameter required is the *CV* parameter (which can be estimated directly from data collected in field experiments such as those summarized in Figure 2). Note also that snow covered area can be estimated from the probability distribution using computationally efficient analytical approaches.

4. Importance of Adequately Parameterizing Spatial Variability Below the Resolved Model Scale: A Case Study From a Mountain Catchment in the Southern Alps, New Zealand

[42] The paper now shifts to examine the multiscale spatial variability in snow depth, as collected in a field campaign in the New Zealand mountains, in order to investigate the suitability of alternative modeling approaches.

4.1. Field Campaign

[43] Data on the spatial variability of snow depth was collected in the upper Jollie Catchment, in the central Southern Alps of New Zealand (Figure 6). The study area is approximately 30 km^2 in area with a minimum elevation of 1067 m and maximum elevation of 2726 m. Slope angles range from 0° to 62°, with a mean slope angle for the catchment of 33° (as derived from a 30 m Digital Elevation Model). The area is made up of two main valley systems, the Jollie and the Pinnacle, which are both oriented approximately NE-SW (Figure 6). The study area is covered in tussocks and various low lying alpine plants and mosses at lower elevation (below 1400 m) and is mainly bare rock and talus at high elevations. The catchment is in the rain shadow of the New Zealand Southern Alps, and precipitation totals in the Pinnacle Stream have been measured at ~2000 mm yr^{-1}. The Jollie River is a tributary of the Tasman River, which flows into Lake Pukaki, one of New Zealand's major hydro electricity generation lakes. Snow in New Zealand can be characterized as being maritime in nature [*Sturm et al.*, 1995; *Owens et al.*, 2004].

[44] Data was collected by eight separate groups on the 20 September 2007. This date is representative of conditions near the end of the accumulation season. The field campaign used helicopters to deploy groups throughout the upper Jollie catchment. Four groups were positioned on ridgelines, while four more teams were positioned in the two valleys. Each group collected snow depth and density data along specified transects. Using a standard avalanche probe, five snow depths were taken within a 0.5 m × 0.5 m area at each location. Sets of snow depth observations (locations) were taken every 10 m along the contour to create a transect. Each group started a different transect every 100–200 vertical meters (Figure 6). In total, 2035 snow depth measurements (5 measurements at 407 locations) were made over 26 transects. In some cases field personnel were unable to probe to the base of the snowpack; in these cases the snow depth was recorded as the maximum depth measured (the maximum length of the probe plus the depth of any snow excavated). At least one observation of snow density was made in each transect. Density was measured using either the Mt. Rose ("Federal") Snow Sampler, or by excavating a snow pit and taking snow density measurements every 0.1 m with depth using a tube sampler and a scale. Each snow depth and snow density measurement location was recorded using a GPS, with accuracy of 5–10 m at most measurement points. In cases of inaccurate GPS readings locations were adjusted based on knowledge of

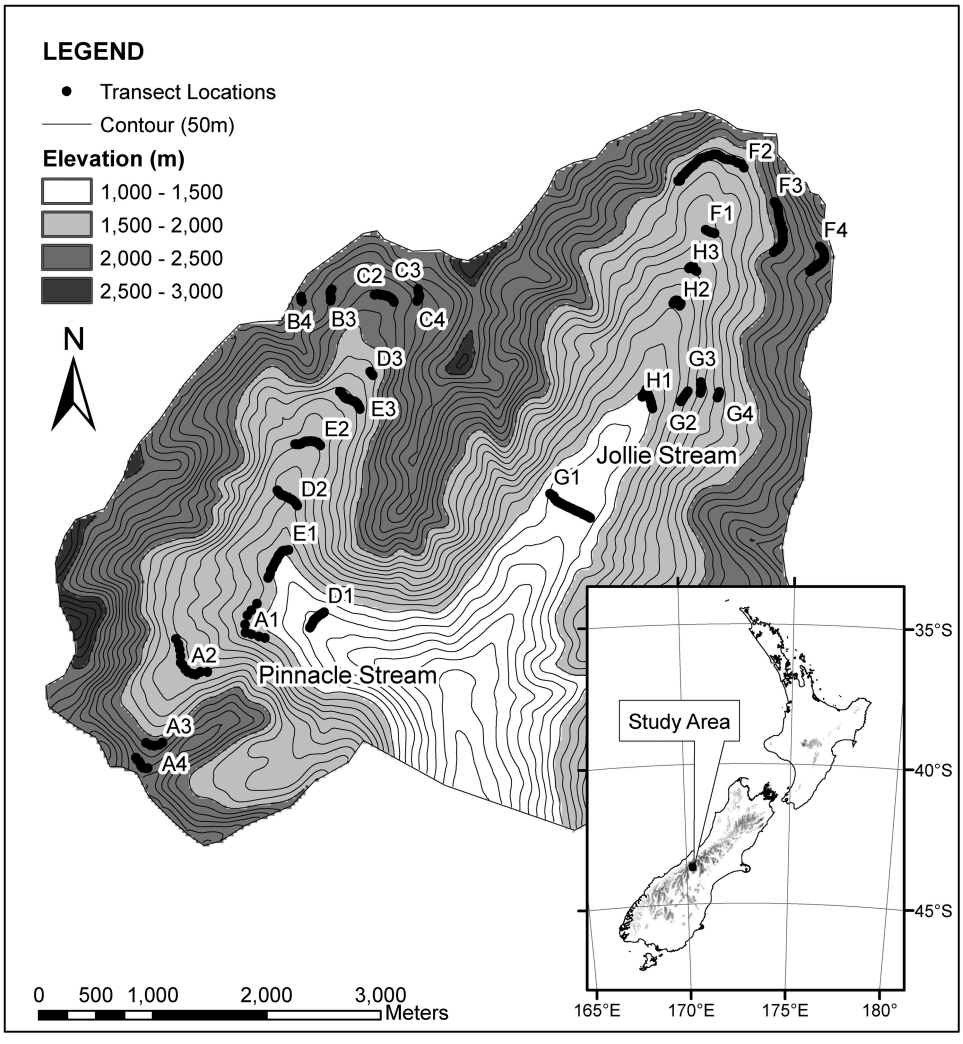

Figure 6. Map of the upper Jollie Catchment showing the location of the 26 transects (black dots). The labels for each transect corresponds to those in Figure 2 and Table 2. Elevations are shaded in 500 m elevation bands and are also shown with contour lines with 50 m intervals. The inset map shows the location of the study area, and uses the same shading to show elevation ranges throughout New Zealand.

the location of the transect, the position of the point within the transect (e.g., the 5th point on the true-left of the center of the transect), and the spacing of measurements. Additional metadata was recorded on surface characteristics, for example, if measurements were taken within avalanche debris.

[45] This measurement strategy provides data on the variability in snow depth at three distinct spatial scales: the point scale (<1 m), as described by the five measurements at each measurement location; the hillslope scale (1–100 m), as described by the variability within each transect; and the watershed scale (100–10,000 m), as described by the variability between all transects.

[46] The analysis in this paper focuses on spatial variability in snow depth (rather than SWE). This is done partly because of the small number of snow density measurements, and partly because snow density did not vary much between transects [see also *Grünewald et al.*, 2010; *Sturm et al.*, 2010]. Snow density was approximately 400 kg m^{-3} in most locations and was relatively uniform with depth (exceptions were in avalanche debris, where snow density was quite difficult to measure).

4.2. Multiscale Variability in Snow Depth

[47] Table 3 presents the results of all snow depth transects. Results show that the probability distribution of snow depth is positively skewed in most transects. This result is consistent with observations in previous studies [e.g., *Shook and Gray*, 1996; *Faria et al.*, 2000; *Marchand and Killingtveit*, 2005] and modeling approaches [*Luce et al.*, 1999; *Liston*, 2004]. Note, however, that most measurements were on slopes less than 40° (Figure 6); given that sloughing and avalanching cause shallow snow on steep slopes, the true probability distribution of snow depth for the basin as a whole is likely to be more positively skewed (and with a higher coefficient of variability) than what is reported in Table 3.

[48] Figure 7 illustrates variograms of snow depth both for (1) all measurement pairs (Figure 7a) and (2) for the

Table 3. Summary Statistics of Snow Depth From Each Transect

Group/Transect	Location	Elevation (m)	Mean	SD	Coefficient Variation	Skewness
A1	Pinnacle (Madonna)	1554	0.70	0.40	0.57	0.42
A2	Pinnacle (Madonna)	1811	0.94	0.55	0.58	0.37
A3	Pinnacle (Madonna)	2044	1.16	0.84	0.73	0.68
A4	Pinnacle (Madonna)	2155	2.10	0.23	0.11	−0.95
B3	Pinnacle (Monk)	2190	2.87	0.15	0.05	−0.50
B4	Pinnacle (Monk)	2303	2.88	1.06	0.37	−0.43
C2	Pinnacle (Abbey Pass)	2091	1.67	0.47	0.28	0.81
C3	Pinnacle (Abbey Pass)	2202	2.10	1.15	0.55	0.36
C4	Pinnacle (Abbey Pass)	2311	2.28	0.85	0.37	−0.61
D2	Pinnacle (valley)	1391	0.28	0.28	0.99	1.16
D3	Pinnacle (valley)	1611	0.76	0.58	0.76	0.99
D4	Pinnacle (valley)	1937	0.93	0.35	0.37	−0.24
E2	Pinnacle (valley)	1508	0.70	0.43	0.61	1.30
E3	Pinnacle (valley)	1704	1.07	0.70	0.65	0.58
E4	Pinnacle (valley)	1846	1.17	0.72	0.61	0.40
F1	Jollie (upper)	1783	1.74	0.92	0.53	0.27
F2	Jollie (upper)	1914	2.00	0.84	0.42	0.17
F3	Jollie (upper)	2048	1.30	0.61	0.47	0.54
F4	Jollie (upper)	2233	1.34	0.79	0.59	1.09
G1	Jollie (east)	1419	0.33	0.21	0.62	0.70
G2	Jollie (east)	1638	0.98	0.77	0.78	0.82
G3	Jollie (east)	1719	0.89	0.22	0.25	1.19
G4	Jollie (east)	1819	0.94	0.41	0.43	0.53
H1	Jollie (valley)	1499	0.47	0.21	0.45	0.68
H2	Jollie (valley)	1616	1.05	0.30	0.28	0.77
H3	Jollie (valley)	1704	1.00	0.37	0.37	0.26

restricted case that only considers measurement pairs within each transect (Figure 7b). The semivariance (γ) at a given spatial scale is computed as

$$\gamma(h) = \frac{1}{2n(h)} \sum_{ij} \left[x_i(h) - x_j(h)\right]^2, \quad (9)$$

where x_i and x_j are all snow depth values at a given lag distance h, and n is the number of data points at a given distance h.

[49] To construct the variogram we ranked all data pairs in terms of distance, and identified a set of distance categories, each with the same number of data pairs ($n = 498$ for all data pairs, and $n = 259$ for the restricted case that only considers measurement pairs within each transect). For each category, we computed the semivariance and the mean of the distances in that category.

[50] Figure 7 illustrates some interesting characteristics in the variability in snow depth. When all distance pairs are considered, the variance increases with spatial scale (Figure 7a). The spatial variance is largest at horizontal scales of ~3000 m, as it is this scale where elevation differences are maximized (see Figure 6). However, when restricting attention to distance pairs *within each transect* (i.e., filtering out the effects of elevation), the data suggests that the spatial variability is dominant at horizontal scales of 50–100 m.

[51] Figure 8 illustrates the relationship between elevation and variability in snow depth *between* transects. While there is a clear relationship between snow depth and elevation, several outliers are apparent. At least in some cases, these outliers can be explained by local conditions. For example, (1) Group F's transect at 1913 m (F2) was immediately below a cliff band, and snow depth was significantly higher in this region due to the effects of sloughing and avalanching; (2) the high snow depths recorded by group B

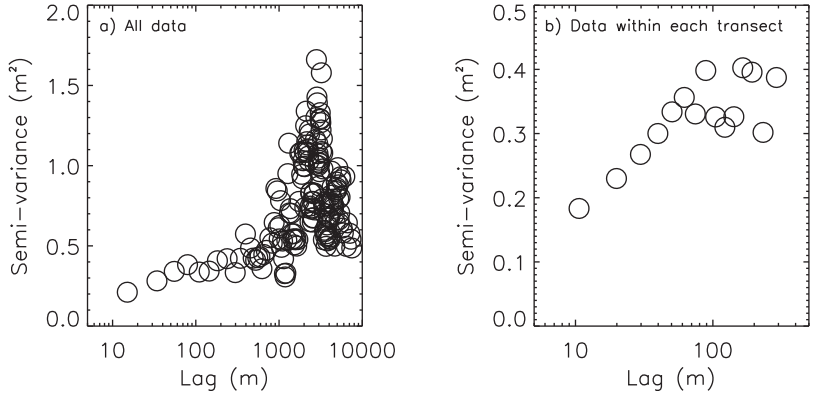

Figure 7. Spatial variograms of depth, showing (a) all possible data pairs and (b) only data pairs within the same transect.

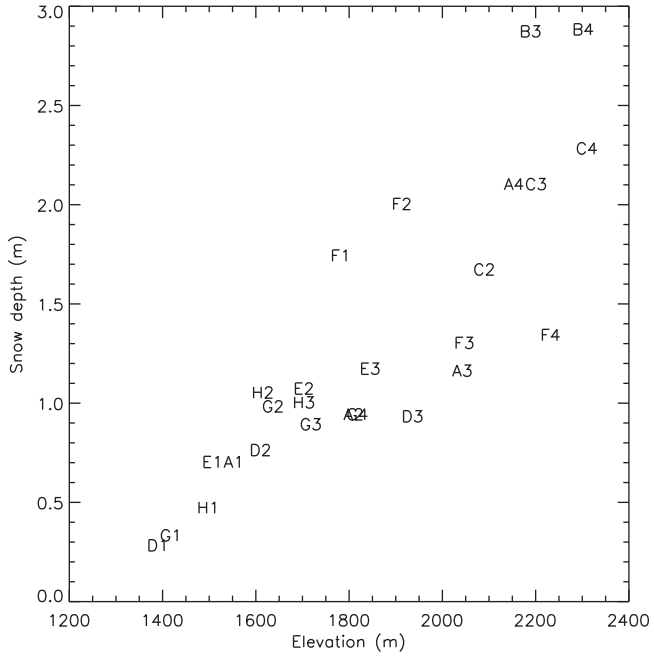

Figure 8. Relationship between elevation and transect-average snow depth in the Jollie River basin. The codes refer to different transects (see Table 2 for more details). Note that the symbols A2 and G4 overlap.

were located on Monk Glacier and may reflect locally high areas of snow accumulation in the lee of the prevailing westerly winds; and (3) some transects have only a small number of measurements, e.g., transect F1 was relatively short and dominated by deep snow drifts on the valley side. Note also that the relationship between elevation and transect-average snow depth deteriorates at higher elevations, especially for elevation ranges less than ~200 m. A likely explanation for the relationship between elevation and snow depth is that large-scale spatial variability in freezing levels and melt energy control large-scale spatial variability in snow depth.

4.3. Synopsis

[52] The field data illustrates multiscale spatial variability in snow depth, with spatial variability shaped by a range of different processes that occur across a hierarchy of spatial scales. The clear impacts of elevation on spatial variability of depth are associated with spatial variability in freezing levels and melt energy. Such variability can be represented directly in a spatially distributed model through spatial interpolation of the model forcing data. The spatial variability at scales less than 100 m is associated with preferential snow deposition in small hollows and in the lee of obstacles such as boulders and ridges, scouring of snow off exposed areas and redeposition of snow in sheltered areas, sloughing of snow off steep slopes, and avalanching. These processes are difficult to model directly, and therefore, the suggestion of statistical homogeneity in Figure 7 is important because it supports the use of probability distributions to approximate the aggregate impact of snow processes operating below the resolved model scale of ~100 m.

[53] The multiscale variability in snow depth identified here is dependent on both the experimental design (e.g., we sampled snow depths over a sufficiently large elevation range such that the elevation relationship is discernable), and the landscape and climate (e.g., elevation is an important control because temperatures are close to the freezing point during winter, and the steep terrain has a large impact on variability at the hillslope scale). We stress that the conclusions have been drawn from analysis at a single valley and, moreover, represent a snapshot of spatial variability in snow depth on one day. Moreover, the end-of-winter snow survey biases results toward emphasizing the spatial variability of snow depth caused by accumulation processes, although midwinter melt is also important, especially at lower elevations. Further measurements throughout the melt season are needed to better understand the spatial variability caused by melt processes (e.g., controls by radiation loading associated with differences in aspect). In spite of these limitations, the spatial variability documented in the Jollie is consistent with results from many previous studies, and provides a useful case study to evaluate the design of distributed snow models.

5. Model Sensitivity Experiments

5.1. Model Configurations

[54] The impact of model scale is assessed using a suite of sensitivity experiments with a relatively simple energy balance snow model, applied to the Pinnacle Stream subcatchment (12.5 km^2). The snow model used is similar in structure to that described by *Tarboton and Luce* [1996] and is forced with interpolated climate data produced using the methods described in the work of *Tait et al.* [2006], adjusted to match the elevation and aspect of each

model element. The spatial variability of the snow accumulation is generated in an idealized fashion that is intended to represent the observed spatial variability but not the observed location of shallow and deep snow. The sensitivity experiments are designed to illustrate how different process representations and modeling scales affect model outputs.

[55] The following model configurations are trialed (see Table 4 for details on the spatial adjustment of forcing data):

[56] 1. Explicit resolution of watershed-scale variability. Watershed-scale variability is resolved by disaggregating the catchment into smaller grid cells or elevation bands, and using different snow model inputs (e.g., solar radiation, temperature) for each grid cell or elevation band. Two spatial setups were tested: (1) vertical discretization, where the Pinnacle Stream subcatchment is disaggregated into elevation bands (a single elevation band is included in this case, which represents a spatially lumped representation); and (2) areal discretization, where the Pinnacle Stream subcatchment is disaggregated to 5×5, 10×10, 50×50, and 100×100 m grids.

[57] For the case of elevation bands the temperature inputs to the model are extrapolated to each grid cell or elevation band using the lapse rate of 5 K km^{-1} (which is appropriate for the high humidity environment [*Norton*, 1985]), and for the case of grid cells temperature is adjusted in an identical manner as for elevation bands but also the solar radiation inputs to the model are adjusted based on the solar incidence angle (Table 4). Specific humidity, wind speed, and incoming longwave radiation were held spatially constant for all model experiments. Such spatial disaggregation accounts for watershed-scale variability associated with spatial differences in freezing levels and melt energy.

[58] 2. Explicit resolution of hillslope-scale variability. Hillslope-scale variability is simulated using spatially correlated redistribution multipliers [*Luce et al.*, 1998], applied to the 5 m $\times$ 5 m grid. In this approach snow accumulation is reduced over areas with low multipliers and increased in areas with high multipliers. While *Luce et al.* [1998] define multipliers based on gridded observations, we were unable to sample snow over a regular grid, and multipliers must be defined statistically using spatially correlated random numbers. The use of random numbers means that although the overall spatial variability is similar to our observations, the exact location of deep snow drifts is random. The spatial correlation function used in the random number generator was defined as

$$c(d) = c_0 \exp\left(-\frac{d}{c_{\text{len}}}\right), \tag{10}$$

where $c(d)$ is the correlation at a specified distance d (m), c_0 is the small-scale correlation (the "nugget"), and c_{len} is the correlation length scale (m), which, to be consistent with results presented in Figure 7, are specified as $c_0 = 0.75$ and $c_{\text{len}} = 50$ m. The spatially correlated fields were generated using the method described by *Clark and Slater* [2006]. The redistribution multipliers for the 10×10, 50×50 and 100×100 m grids were obtained by spatially averaging the multipliers from the 5 m $\times$ 5 m grid.

[59] 3. Implicit representation of unresolved variability. The spatial variability within a model element is simulated using the parameterization of *Luce et al.* [1999] and *Liston* [2004], where subgrid variability *due to accumulation processes* is modeled using a two-parameter probability distribution, where the mean of the distribution is equal to the total snow accumulation and the coefficient of variation is a model parameter that must be specified (here the coefficient of variation parameter is set at 1.0). This probability distribution describes the aggregate impact of processes below the model element size. As noted in section 4, both *Luce et al.* [1999] and *Liston* [2004] assume that snow melt is uniform throughout the model element. This means that shallow areas of snow melt first, resulting in a reduction of snow coverage over the model element and corresponding reductions in snowmelt-runoff for the model element as a whole.

5.2. Model Results

[60] Figure 9 illustrates the SWE simulations for each of the model configurations. Several features are immediately apparent:

[61] 1. Explicitly resolving watershed-scale variability *using elevation bands* has a pronounced impact on the rate of snow melt; as expected, the basin average melt rate (average of all elevation bands) is much lower than the melt rate at the mean basin elevation, especially toward the end of the season when snow is only present at higher elevations. This emphasizes the increasing influence of snow covered area on basin average melt as the melt season progresses, and suggests that the spatially lumped simulations inadequately represent the nonlinear relationships between snow melt and elevation. Similar sensitivities are demonstrated by *Lundquist and Dettinger* [2004].

[62] 2. Explicitly resolving watershed-scale variability *using grid cells* explicitly accounts for the spatial variability in solar loading, and hence results in minor differences in snow melt when compared to the spatial discretization using elevation bands (Figure 9b). Larger differences between simulations of SWE using grid cells versus elevation bands may occur if we used different experimental configurations, e.g., if we generated spatially variable wind fields to account for spatial differences in turbulent heat fluxes, or if we included the effects of terrain shading on incoming shortwave radiation. The gridded simulations on

Table 4. Adjustment of Model Inputs for Each Model Configuration

Model Configuration	Precipitation	Solar Radiation	Temperature
Spatially lumped	spatially constant	spatially constant	spatially constant
Elevation bands	spatially constant	spatially constant	extrapolate using lapse rate of 5° km^{-1}
Horizontal grid (no redistribution)	spatially constant	adjust based on solar incidence angle	extrapolate using lapse rate of 5° km^{-1}
Horizontal grid (redistribution)	use redistribution multipliers	adjust based on solar incidence angle	extrapolate using lapse rate of 5° km^{-1}

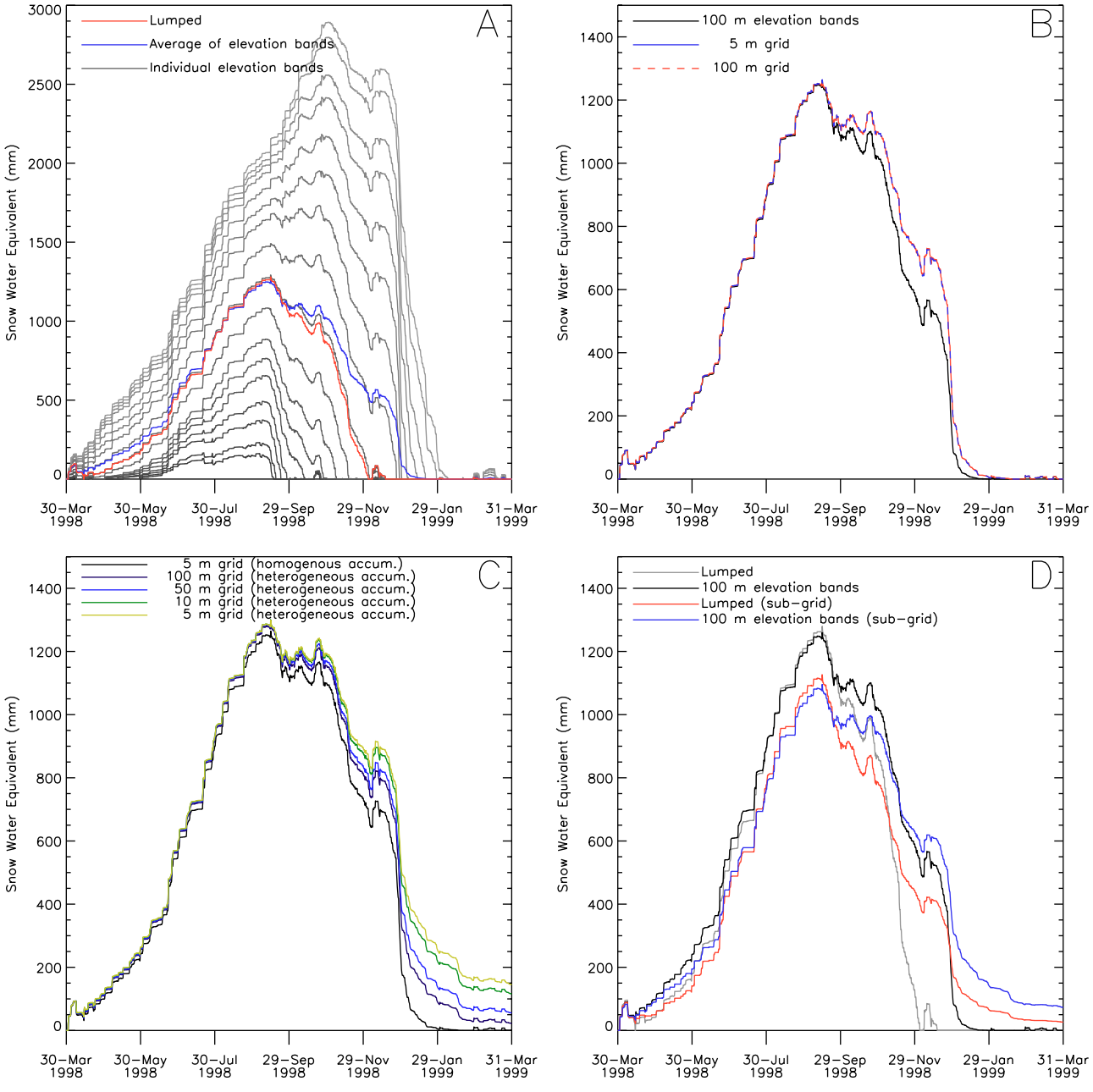

Figure 9. Seasonal evolution of SWE for different model configurations, showing (a) SWE in each individual elevation band compared with the basin-average SWE (averaged across all elevation bands) and SWE from the spatially lumped representation; (b) basin-average SWE computed using 100-m elevation bands, compared with SWE computed using 100 m and 5 m horizontal grids; (c) basin-average SWE computed using a 5 m horizontal grid and homogenous accumulation, compared with basin-average SWE at different grid resolutions with heterogeneous accumulation; and (d) basin-average SWE both with and without vertical discretization (lumped simulations versus 100 m elevation bands), compared with basin-average SWE both with and without subgrid SWE representations. Note that Figure 9a has a different vertical scale.

the 5 and 100 m resolutions are indistinguishable, because the model configurations at finer spatial scales do not explicitly include any additional small-scale processes and the spatial discretization errors appear small at this resolution.

[63] 3. Explicitly resolving the impact of hillslope-scale variability (e.g., as associated with nonhomogenous precipitation distribution, drifting, sloughing, and avalanching), substantially increases the duration of snow in the model (Figure 9c), especially at 10 and 5 m resolutions where the hillslope-scale variability has not been averaged out.

[64] 4. Parameterizing subgrid processes using probability distributions increases the duration of snow in the model (Figure 9d). However, implicitly resolving subgrid variability in the lumped simulations does not simulate the

persistence of snow at high elevations, and hence results in much earlier melt out than the spatially explicit simulations (Figure 9d). It is, of course, possible to extend the duration of the snow season in lumped model configurations by increasing the coefficient of variability parameter (see Figures 3 and 4), but the general applicability of this approach is questionable for basins with large elevation gradients because of the thresholds associated with snow accumulation and melt are difficult to resolve with continuous probability distributions. The use of the subgrid probability distributions in conjunction with elevation bands increases the duration of snow in the model in a similar manner to the spatially explicit simulations with redistribution multipliers on a 5 m $\times$ 5 m grid (compare Figure 9d with Figure 9c).

[65] Section 5.3 discusses the implications of these results for model design.

5.3. Definition of the Model Scale

[66] Ideally, snow model simulations should be produced at the spatial scale where hillslope-scale processes are clearly distinguishable from watershed-scale processes. If the spatial scale of discrete model elements is too small, then some hillslope-scale processes will need to be explicitly represented in the model; if the spatial scale of the model is too large, then some watershed-scale processes will need to be implicitly resolved by the model. For example, as shown in Figure 9, it may be a poor choice to produce model simulations for a 50 m $\times$ 50 m grid, as the processes at the hillslope scale will have to be both explicitly resolved by the model *and* represented as a continuous function.

[67] Variability in snow depth is caused by a mix of multiple processes with different relative importance at different spatial scales [see also *Seyfried and Wilcox*, 1995]. Results from this investigation show there is substantial variability at spatial scales less than 100 m (e.g., Figure 7). Similar results are evident in previous studies [e.g., *Shook and Gray*, 1996; *Lapen and Martz*, 1996; *Luce et al.*, 1998, 1999; *Erxleben et al.*, 2002; *Winstral et al.*, 2002; *Erickson et al.*, 2005; *Deems et al.*, 2006; *Trujillo et al.*, 2007; *Lehning et al.*, 2008; *Dadic et al.*, 2010; *Mott et al.*, 2011; Schirmer et al., submitted manuscript, 2011]. Results from this study also show that elevation alone is a poor predictor for snow depth at elevation intervals less than 200 m (e.g., Figure 8), providing further evidence of the importance of hillslope-scale processes. Similar results are also evident in previous studies; for example, the measurements in the work of *Anderton et al.* [2004] span an elevation range of only 215 m, and elevation did not emerge as a predictor of snow depth. However, spatial differences in freezing levels and melt energy do dominate over other processes at spatial scales greater than $\sim$200 m, as evident in the strong relationship between elevation and snow depth that is obtained when the hillslope-scale variability has been "averaged out" (Figure 8). Again, this result is evident in previous studies [e.g., *Blöschl and Kirnbauer*, 1992; *Elder et al.*, 1998; *Watson et al.*, 2006].

[68] A noteworthy result from this study is that an extremely fine horizontal grid (e.g., 5 m $\times$ 5 m) is necessary to *explicitly* resolve variability at the hillslope scale. This imposes a substantial computational burden. These results are consistent with the model simulations of preferential deposition and snow transport presented by *Mott and Lehning* [2010], where they demonstrated that a 5 m grid increment is necessary to reproduce the smaller-scale deposition features such as dunes and cornices that are shaped by snow transport processes. In spite of these new modeling capabilities, *Mott et al.* [2011] demonstrated through scaling analysis that a 5 m grid increment is still insufficient to resolve the full range of spatial scales associated with drifting processes; indeed, other processes such as sloughing of snow of steep slopes may be difficult to simulate directly. Moreover, in other snow environments (e.g., shrub and forest) explicitly resolving processes such as trapping of snow by shrubs and the nonuniform unloading of snow by the forest canopy is a very difficult proposition.

[69] Subgrid probability distributions produce effective simulations of the aggregate impact of hillslope-scale processes, and this is a viable alternative for many applications. The sensitivity experiments demonstrate that while subgrid probability distributions are effective at the hillslope scale, they may not adequately represent the spatial variability across large elevation gradients. In regions of complex terrain snow accumulation and melt processes are dominated by sharp thresholds that are difficult to resolve with continuous probability distributions. Moreover, the relationship between snow melt and elevation does not support the assumption of uniform melt over a model element. In such cases, it may be more appropriate to resolve spatial variability at the watershed scale through spatial discretization of the model domain into smaller computational elements.

6. Summary

[70] This paper uses field data on the spatial variability of SWE to guide the design of distributed snow models. Model design strategies are gleaned from a reanalysis of results from previous field studies, from analysis of field data on spatial variability of snow collected in a rugged mountain catchment in the Southern Alps, New Zealand, and from model sensitivity experiments.

[71] In most environments, variability in snow depth is caused by a mix of different processes that occur at different spatial scales. Variability in snow depth depends on the landscape and vegetation; scour and redeposition of snow by wind is important in the prairies, interception, and sublimation of snow by the forest canopy (and spatial variability of radiative fluxes within the forest canopy) is important in the boreal forest, and trapping of snow by shrubs is important in the sub-Arctic tundra. In mountain environments many processes act simultaneously to cause variability in snow depth. The dominant processes *at the hillslope-scale* (1–100 m) are preferential deposition in sheltered areas, scour and redeposition of snow by wind, sloughing and avalanching, and, where trees are present, interception and sublimation of snow by the forest canopy and spatial variability of radiative fluxes within the forest canopy. In maritime mountain environments the spatial variability in end-of-winter snow accumulation *at the watershed scale* (100–10,000 m) is additionally dictated by the spatial variability in freezing levels and melt energy.

[72] Analysis of field data from the Jollie catchment in the New Zealand Southern Alps shows that spatial variability has different properties across multiple spatial scales.

Spatial variability is quite pronounced at spatial scales less than ~100 m. When these hillslope-scale variations are averaged out, there is a strong relationship between elevation and snow depth, suggesting that large-scale spatial variability in freezing levels and melt energy control watershed-scale spatial variability in SWE. A key modeling challenge is to adequately represent spatial variability across this hierarchy of spatial scales.

[73] The model sensitivity experiments provide some guidance for model design. Explicitly resolving hillslope-scale variability in simulation models requires an extremely fine horizontal grid, and hence large computational resources. However, subgrid probability distributions produce effective simulations of the aggregate impact of hillslope-scale processes, and this is a viable alternative for many applications. The sensitivity experiments also demonstrate that while subgrid probability distributions are effective at the hillslope scale, they may not adequately represent the spatial variability across large elevation gradients. In such cases, it may be more appropriate to resolve spatial variability at the watershed scale through spatial discretization of the model domain into smaller computational elements.

[74] Our guidance for model design must be viewed in context of the incredible diversity of modeling applications. The design of a model depends first and foremost on the purpose of the modeling exercise but also on the data that is available, computational resources, and the type of environment where the model is applied. It is therefore difficult if not impossible to prescribe a generic spatial configuration for snow models, and that is not our intent. We rather hope that the synthesis of data on the spatial variability of snow in different environments, along with demonstration of different ways of accounting for spatial variability in models, will help other investigators design a modeling strategy that is suitable for their specific applications.

[75] **Acknowledgments.** We thank Ethan Guttman, Jessica Lundquist, and (in particular) Matt Sturm for their constructive comments on an earlier version of this manuscript. We are also grateful to the following people for their help with the snow measurements: Gab Abramowitz, Yvonne Baeuerle, Euan Boyd, Craig Cardie, Ngaio Fletcher, Reece Geursen, Sarah Gillet, Penny Goddard, David Hood, Lawrence Kees, Gerrit Kopmann, Rasmus Kulseng, Mette Riger-Kusk, Ben Mason, Michael Orton, Shane Rodwell, Pascal Sirguey, Claire Sims, Ian Smith, Nita Smith, Amber Tate, and Sam Taylor. Portions of this research were supported by NOAA (NA06OAR4310065) and NASA (NNG06GH10G).

References

Anderton, S. P., S. M. White, and B. Alvera (2004), Evaluation of spatial variability in snow water equivalent for a high mountain catchment, *Hydrol. Processes*, *18*, 435–453.

Balk, B., and K. Elder, (2000), Combining binary decision tree and geostatistical methods to estimate snow distribution in a mountain watershed, *Water Resour. Res.*, *36*, 13–26, doi:10.1029/1999WR900251.

Blöschl, G. (1999), Scaling issues in snow hydrology, *Hydrol. Processes*, *13*, 2149–2175.

Blöschl, G., and R. Kirnbauer (1992), An Analysis of snow cover patterns in a small alpine catchment, *Hydrol. Processes*, *6*, 99–109.

Blöschl, G., and M. Sivapalan (1995), Scale issues in hydrological modelling—A review, *Hydrol. Processes*, *9*, 251–290.

Blöschl, G., R. Kirnbauer, and D. Gutknecht (1991a), Distributed snowmelt simulations in an alpine catchment, 1. Model evaluation of the basis of snow cover patterns, *Water Resour. Res.*, *27*, 3171–3179, doi:10.1029/91WR02250.

Blöschl, G., D. Gutknecht, and R. Kirnbauer (1991b), Distributed snowmelt simulations in an alpine catchment, 2. Parameter study and model predictions, *Water Resour. Res.*, *27*, 3180–3188, doi:10.1029/91WR02251.

Blöschl, G., R. B. Grayson, and M. Sivapalan (1995), On the representative elementary area (REA) concept and its utility for distributed rainfall-runoff modeling, *Hydrol. Processes*, *9*, 313–330.

Bruland, O., K. Sand, and A. Killingtveit (2001), Snow distribution at a high arctic site in Svalbard, *Nord. Hydrol.*, *32*, 1–12.

Bruland, O., G. E. Liston, J. Vonk, K. Sand, and A. Killingtveit (2004), Modelling the snow distribution at two high arctic sites at Svalbard, Norway, and at an alpine site in central Norway, *Nord. Hydrol.*, *35*, 191–208.

Buttle, J. M., and J. J. McDonnell (1987), Modeling the areal depletion of snowcover in a forested catchment, *J. Hydrol.*, *90*, 43–60.

Cess, R. D., et al. (1991), Interpretation of snow-climate feedback as produced by 17 general-circulation models, *Science*, *253*, 888–892.

Clark, M. P., and A. G. Slater (2006), Probabilistic quantitative precipitation estimation in complex terrain, *J. Hydrometeorol.*, *7*(1), 3–22.

Cline, D., et al. (2009), NASA Cold Land Processes Experiment (CLPX 2002/03): Airborne remote sensing, *J. Hydrometeorol.*, *10*, 338–346.

Dadic, R., R. Mott, M. Lehning, and P. Burlando (2010), Wind influence on snow depth distribution and accumulation over glaciers, *J. Geophys. Res.*, *15*, F01012, doi:10.1029/2009JF001261.

Davis, R. E., J. P. Hardy, W. Ni, C. Woodcock, J. C. McKenzie, R. Jordan, and X. Li (1997), Variation of snow cover ablation in the boreal forest: A sensitivity study on the effects of conifer canopy, *J. Geophys. Res.*, *102*(D24), 29,389–29,395, doi:10.1029/97JD01335.

Deems, J. S., S. R. Fassnacht, and K. J. Elder (2006), Fractal distribution of snow depth from Lidar data, *J. Hydrometeorol.*, *7*, 285–297.

Deems, J. S., S. R. Fassnacht, and K. J. Elder (2008), Interannual consistency in fractal snow depth patterns at two Colorado mountain sites, *J. Hydrometeorol.*, *9*, 977–988.

Elder, K., J. Dozier, and J. Michaelsen (1991), Snow accumulation and distribution in an alpine watershed, *Water Resour. Res.*, *27*, 1541–1552, doi:10.1029/91WR00506.

Elder, K., W. Rosenthal, and R. E. Davis (1998), Estimating the spatial distribution of snow water equivalence in a montane watershed, *Hydrol. Processes*, *12*, 1793–1808.

Erickson, T. A., M. W. Williams, and A. Winstral (2005), Persistence of topographic controls on the spatial distribution of snow in rugged mountain terrain, Colorado, United States, *Water Resour. Res.*, *41*, W04014, doi:10.1029/2003WR002973.

Erxleben, J., K. Elder, and R. Davis (2002), Comparison of spatial interpolation methods for estimating snow distribution in the Colorado Rocky Mountains, *Hydrol. Processes*, *16*, 3627–3649.

Essery, R. (1997), Modelling fluxes of momentum, sensible heat and latent heat over heterogeneous snow, *Q. J. R. Meteorol. Soc.*, *123*, 1867–1883.

Essery, R., and J. Pomeroy (2004a), Vegetation and topographic control of wind-blown snow distributions in distributed and aggregated simulations for an Arctic tundra basin, *J. Hydrometeorol.*, *5*, 735–744.

Essery, R., and J. Pomeroy (2004b), Implications of spatial distributions of snow mass and melt rate for snow-cover depletion: Theoretical considerations, *Ann. Glaciol.*, *38*, 261–265.

Essery, R., L. Li, and J. Pomeroy (1999), A distributed model of blowing snow over complex terrain, *Hydrol. Processes*, *13*, 2423–2438.

Faria, D. A., J. W. Pomeroy, and R. L. H. Essery (2000), Effect of covariance between ablation and snow water equivalent on depletion of snow covered area within a forest, *Hydrol. Processes*, *14*, 2683–2695.

Fitzharris, B. B. (1977), Estimating maximum snow storage capacity of central Otago terrain, paper presented at New Zealand Hydrological Society Annual Symposium, N. Z. Hydrol. Soc., Christchurch, NZ.

Geddes, C. I. A., D. G. Brown, and D. B. Fagre (2005), Topography and vegetation as predictors of snow water equivalent across the alpine treeline ecotone at Lee Ridge, Glacier National Park, Montana, USA, *Arc. Antarctic Alpine Res.*, *37*, 197–205.

Greene, E. M., G. E. Liston, and R. A. Pielke (1999), Simulation of above treeline snowdrift formation using a numerical snow-transport model, *Cold Reg. Sci. Technol.*, *30*, 135–144.

Grünewald, T., M. Schirmer, R. Mott, and M. Lehning (2010), Spatial and temporal variability of snow depth and ablation rates in a small mountain catchment, *Cyrosphere*, *4*, 215–225.

Hardy, J. P., R. E. Davis, R. Jordan, X. Li, C. Woodcock, W. Ni, and J. C. McKenzie (1997), Snow ablation modeling at the stand scale in a boreal jack pine forest, *J. Geophys. Res.*, *102*(D24), 29,397–29,405, doi:10.1029/96JD03096.

Harrison, W. (1986), Seasonal accumulation and loss of snow from a block mountain catchment in central Otago, *J. Hydrol. (N.Z.)*, *25*, 1–17.

Homan, J. W., C. H. Luce, J. P. McNamara, and N. F. Glenn (2011), Improvement of distributed snowmelt energy balance modeling with MODIS-based NDSI-derived fractional snow-covered area data, *Hydrol. Processes*, *25*, 650–660, doi:10.1002/hyp.7857.

Hosang, J., and K. Dettwiler (1991), Evaluation of a water equivalent of snow cover map in a small catchment using a geostatistical approach, *Hydrol. Processes*, *5*, 283–290.

Iacozza, J., and D. G. Barber (1999), An examination of the distribution of snow on sea ice, *Atmos. Ocean*, *17*, 21–51.

Jost, G., M. Weiler, D. R. Gluns, and Y. Alila (2007), The influence of forest and topography on snow accumulation and melt at the watershed-scale, *J. Hydrol.*, *347*, 101–115.

König, M., and M. Sturm (1998), Mapping snow distribution in the Alaskan Arctic using aerial photography and topographic relationships, *Water Resour. Res.*, *34*, 3471–3483, doi:10.1029/98WR02514.

Kuchment, L. S., and A. N. Gelfan (2001), Statistical self-similarity of spatial variations in snow cover: Verification of the hypothesis and application in snowmelt runoff generation models, *Hydrol. Processes*, *15*, 3343–3345.

Kumar, P. (2011), Typology of hydrologic predictability, *Water Resour. Res.*, *47*, W00H05, doi:10.1029/2010WR009769.

Kuusisto, R. (1980), On the values and variability of the degree-day melting factor in Finland, *Nord. Hydrol.*, *11*, 235–242.

Lapen, D. R., and L. W. Martz (1996), An investigation of the spatial association between snow depth and topography in a prairie agricultural landscape using digital terrain analysis, *J. Hydrol.*, *184*, 277–298.

Lehning, M., H. Lowe, M. Ryser, and N. Raderschall (2008), Inhomogeneous precipitation distribution and snow transport in steep terrain, *Water Resour. Res.*, *44*, W07404, doi:10.1029/2007WR006545.

Link, T. E., and D. Marks (1999a), Point simulation of seasonal snow cover dynamics beneath boreal forest canopies, *J. Geophys. Res.*, *104*(D22), 27,841–27,857, doi:10.1029/1998JD200121.

Link, T., and D. Marks (1999b), Distributed simulation of snowcover mass- and energy-balance in the boreal forest, *Hydrol. Processes*, *13*, 2439–2449.

Liston, G. E. (1995), Local advection of momentum, heat, and moisture during the melt of patchy snow covers, *J. Appl. Meteorol.*, *34*, 1705–1715.

Liston, G. E. (1999), Interrelationships among snow distribution, snowmelt, and snow cover depletion: Implications for atmospheric, hydrologic, and ecologic modelling, *J. Appl. Meteorol.*, *38*, 1474–1487.

Liston, G. E. (2004), Representing subgrid snow cover heterogeneities in regional and global models, *J. Clim.*, *17*, 1381–1397.

Liston, G. E., and M. Sturm (2002), Winter precipitation patterns in arctic Alaska determined from a blowing-snow model and snow-depth observations, *J. Hydrometeorol.*, *3*, 646–659.

Luce, C. H., and D. G. Tarboton (2004), The application of depletion curves for parameterization of subgrid variability of snow, *Hydrol. Processes*, *18*, 1409–1422.

Luce, C. H., D. G. Tarboton, and K. R. Cooley (1998), The influence of the spatial distribution of snow on basin-averaged snowmelt, *Hydrol. Processes*, *12*, 1671–1683.

Luce, C. H., D. G. Tarboton, and K. R. Cooley (1999), Sub-grid parameterization of snow distribution for an energy and mass balance snow model, *Hydrol. Processes*, *13*, 1921–1933.

Lundquist, J. D., and M. Dettinger (2005), How snowpack heterogeneity affects diurnal streamflow timing, *Water Resour. Res.*, *41*, W05007, doi:10.1029/2004WR003649.

Lundquist, J. D., M. Dettinger, and D. Cayan (2005), Snow-fed streamflow timing at different basin scales: Case study of the Tuolumne River above Hetch Hetchy, Yosemite, California, *Water Resour. Res.*, *41*, W07005, doi:10.1029/2004WR003933.

Machguth, H., O. Eisen, F. Paul, and M. Hoelzle (2006), Strong spatial variability of snow accumulation observed with helicopter-borne GPR on two adjacent alpine glaciers, *Geophys. Res. Lett.*, *33*, L13503, doi:10.1029/2006GL026576.

Marchand, W., and A. Killingtveit (2005), Statistical probability distribution of snow depth at the model sub-grid cell spatial scale, *Hydrol. Processes*, *19*, 355–369.

Marks, D., M. Reba, J. Pomeroy, T. Link, A. Winstral, G. Flerchinger, and K. Elder (1998), Comparing simulated and measured sensible and latent heat fluxes over snow under a pine canopy to improve an energy balance snowmelt model, *J. Hydrometeorol.*, *9*, 1506–1522.

McCartney, S. E., S. K. Carey, and J. W. Pomeroy (2006), Intra-basin variability of snowmelt water balance calculations in a subarctic catchment, *Hydrol. Processes*, *20*, 1001–1016.

Mott, R., and M. Lehning (2010), Meteorological modeling of very high-resolution wind fields and snow deposition for mountains, *J. Hydrometeorol.*, *11*, 934–949.

Mott, R., M. Schirmer, and M. Lehning (2011), Scaling properties of wind and snow depth distribution in an alpine catchment, *J. Geophys. Res.*, *116*, D06106, doi:10.1029/2010JD014886.

Murray, C. D., J. M. Buttle (2003), Impacts of clearcut harvesting on snow accumulation and melt in a northern hardwood forest, *J. Hydrol.*, *271*, 197–212.

Niu, G. Y., and Z.-L. Yang (2007), An observation-based formulation of snow cover fraction and its evaluation over large North American river basins, *J. Geophys. Res.*, *112*(D21), D21101, doi:10.1029/2007JD008674.

Norton, D. A. (1985), A multivariate technique for estimating New Zealand temperature normals, *Weather and Climate*, *5*, 64–74.

Owens, I., and B. Fitzharris (2004), Seasonal snow and water, in *Freshwaters of New Zealand, Chap. 6*, edited by J. Harding et al., Caxton Press, Christchurch, New Zealand.

Pomeroy, J. W., D. M. Gray, and P. G. Landine (1993), The prairie blowing snow model – Characteristics, validation, operation, *J. Hydrol.*, *144*, 165–192.

Pomeroy, J. W., D. M. Gray, K. R. Shook, B. Toth, R. L. H. Essery, A. Pietroniro, and N. Hedstrom (1998), An evaluation of snow accumulation and ablation processes for land surface modeling, *Hydrol. Processes*, *12*, 2339–2367.

Pomeroy, J. W., D. M. Gray, N. R. Hedstrom, and J. R. Janowicz (2002), Prediction of seasonal snow accumulation in cold climate forests, *Hydrol. Processes*, *16*, 3543–3558.

Pomeroy, J., R. Essery, and B. Toth (2004), Implications of spatial distributions of snow mass and melt rate for snow-cover depletion: Observations in a subarctic mountain catchment, *Ann. Glaciol.*, *38*, 195–201.

Pomeroy, J. W., D. S. Bewley, R. L. H. Essery, N. R. Hedstrom, T. Link, R. J. Granger, J. E. Sicart, C. R. Ellis, and J. R. Janowicz (2006), Shrub tundra snowmelt, *Hydrol. Processes*, *20*, 923–941.

Pomeroy, J., A. Rowlands, J. Hardy, T. Link, D. Marks, R. Essery, J. E. Sicart, and C. Ellis (2008), Spatial variability of shortwave irradiance for snowmelt in forests, *J. Hydrometeorol.*, *9*, 1482–1490.

Roesch, A., M. Wild, H. Gilgen, and A. Ohmura (2001), A new snow cover fraction parametrization for the ECHAM4 GCM, *Clim. Dyn.*, *17*, 933–946.

Seyfried, M. S., and B. P. Wilcox (1995), Scale and the nature of spatial variability: Field examples having implications for hydrologic modeling, *Water Resour. Res.*, *31*, 173–184, doi:10.1029/94WR02025.

Shanley, J. B., and A. Chalmers (1999), The effect of frozen soil on snowmelt runoff at Sleepers River, Vermont, *Hydrol. Processes*, *13*, 1843–1857.

Shook, K., and D. M. Gray (1996), Small-scale spatial structure of shallow snow covers, *Hydrol. Processes*, *10*, 1283–1293.

Sicart, J. E., J. W. Pomeroy, R. L. H. Essery, J. Hardy, T. Link, and D. Marks (2004), A sensitivity study of daytime net radiation during snowmelt to forest canopy and atmospheric conditions, *J. Hydrometeorol.*, *5*, 774–784.

Skaugen, T. (2007), Modelling the spatial variability of snow water equivalent at the catchment scale, *Hydrol. Earth Syst. Sci.*, *11*, 1543–1550.

Skoien, J. O., and G. Blöschl (2006), Sampling scale effects in random fields and implications for environmental monitoring, *Environ. Monit. Assess.*, *114*, 521–552.

Sturm, M. (1992), Snow distribution and heat flow in the taiga, *Arct. Alp. Res.*, *24*, 145–152.

Sturm, M., and G. E. Liston (2003), The snow cover on lakes of the Arctic Coastal Plain of Alaska, USA, *J. Glaciol.*, *49*, 370–380.

Sturm, M., J. Holmgren, and G. E. Liston (1995), A Seasonal Snow Cover Classification System for Local to Global Applications, *J. Clim.*, *8*, 1261–1283.

Sturm, M., K. Morris, and R. Massom (1998), The winter snow cover on the west Antarctic pack ice: Its spatial and temporal variability, in *Antarctic Sea Ice: Physical Processes, Interactions, and Variability, Antarct. Res. Ser.*, *74*, 1–18.

Sturm, M., Liston, G. E., C. S. Benson, and J. Holmgren (2001a), Characteristics and growth of a snowdrift in arctic Alaska, USA, *Arct. Antarct. Alp. Res.*, *33*, 319–329.

Sturm, M., J. P. McFadden, G. E. Liston, F. S. Chapin, C. H. Racine, and J. Holmgren (2001b), Snow-shrub interactions in Arctic tundra: A hypothesis with climatic implications, *J. Clim.*, *14*, 336–344.

Sturm, M., J. Holmgren, and D. K. Perovich (2002), Winter snow cover on the sea ice of the Arctic Ocean at the Surface Heat Budget of the Arctic

Ocean (SHEBA): Temporal evolution and spatial variability, *J. Geophys. Res.*, *107*(C10), 8047, doi:10.1029/2000JC000400.

Sturm, M., B. Taras, G. E. Liston, C. Derksen, T. Jonas, and J. Lea (2010), Estimating snow water equivalent using snow depth data and climate classes, *J. Hydrometeorol.*, *11*, 1380–1394.

Tait, A., R. Henderson, R. Turner, and X. Zheng (2006), Thin-plate smoothing spline interpolation of daily rainfall for New Zealand using a climatological rainfall surface, *Int. J. Climatol.*, *26*, 2097–2115.

Tarboton, D. G., and C. H. Luce (1996), Utah energy balance snow accumulation and melt model (UEB), Computer model technical description and users guide, Utah Water Res. Lab. and USDA For. Serv. Intermountain Res. Station, Logan, Utah.

Trujillo, E., J. A. Ramirez, and K. J. Elder (2007), Topographic, meteorologic, and canopy controls on the scaling characteristics of the spatial distribution of snow depth fields, *Water Resour. Res.*, *43*, W07409, doi:10.1029/2006WR005317.

Varhola, A., N. C. Coops, M. Weiler, and R. D. Moore (2010), Forest canopy effects on snow accumulation and ablation: An integrative review, *J. Hydrol.*, *392*, 219–233.

Veatch, W., P. D. Brooks, J. R. Gustafson, and N. P. Molotch (2009), Quantifying the effects of forest canopy cover on net snow accumulation at a continental, mid-latitude site, *Ecohydrology*, *2*, 115–128.

Watson, F. G. R., T. N. Anderson, W. B. Newman, S. E. Alexander, and R. A. Garott (2006), Optimal sampling schemes for estimating snow water equivalents in stratified heterogeneous landscapes, *J. Hydrol.*, *328*, 432–452.

Weir, P. L. (1979), Topographic influences on snow accumulation at Mount Hutt, Master's Thesis, 83 pp., Univ. of Canterbury, Christchurch, New Zealand.

Winkler, R. D., and R. D. Moore (2006), Variability in snow accumulation patterns within forest stands on the interior plateau of British Columbia, Canada, *Hydrol. Processes*, *20*, 3683–3695.

Winstral, A., K. Elder, and R. E. Davis (2002), Spatial snow modelling of wind-redistributed snow using terrain-based parameters, *J. Hydrometeorol.*, *3*, 524–538.

Winther, J. G., O. Bruland, K. Sand, A. Killingtveit, and D. Marechal (1998), Snow accumulation distribution on Spitsbergen, Svalbard, in 1997, *Polar Res.*, *17*, 155–164.

Woo, M. K., and P. Steer (1986), Monte-Carlo simulation of snow depth in a forest, *Water Resour. Res.*, *22*, 864–868, doi:10.1029/WR022i006p00864.

Wood, E. F., M. Sivapalan, K. Beven, and L. Band (1988), Effects of spatial variability and scale with implications to hydrologic modelling, *J. Hydrol.*, *102*, 29–47.

Yang, Z. L., R. E. Dickinson, A. Robock, and K. Y. Vinnikov (1997), Validation of the snow submodel of the biosphere-atmosphere transfer scheme with Russian snow cover and meteorological observational data, *J. Clim.*, *10*, 353–373.

B. Anderson, Antarctic Research Centre, Victoria University of Wellington, PO Box 600, Wellington 6140, New Zealand.

M. P. Clark, National Center for Atmospheric Research, PO Box 3000, Boulder, CO 80307-3000, USA. (mclark@ucar.edu)

N. J. Cullen, Department of Geography, University of Otago, PO Box 56, Dunedin 9054, New Zealand.

J. Hendrikx, Department of Earth Sciences, Montana State University, P.O. Box 3480, Bozeman, MT 59717-3480, USA.

D. Kavetski, Environmental Engineering, University of Newcastle, University Drive, Callaghan, NSW 2308, Australia.

T. Kerr, E. Örn Hreinsson, and R. A. Woods, National Institute of Water and Atmospheric Research, P.O. Box 8602, Christchurch 8011, New Zealand.

A. G. Slater, Cooperative Institute for Research in Environmental Sciences, University of Colorado, Box 216 UCB, Boulder, CO, 80309-216, USA.